minerals

MDPI

Article

Geochemical Features and Mineral Associations of Differentiated Rocks of the Norilsk 1 Intrusion

Nadezhda Tolstykh [1,2,*], Gennadiy Shvedov [3], Aleksandr Polonyankin [4] and Vladimir Korolyuk [1]

1 VS Sobolev Institute of Geology and Mineralogy of Siberian Branch of Russian Academy of Sciences, Koptyuga Prospect., 3, 630090 Novosibirsk, Russia; camebax@igm.nsc.ru
2 Department of Geology and Geophysics, Novosibirsk State University, Pirogova Ave., 2, 630090 Novosibirsk, Russia
3 Institute of Mining, Geology and Geotechnology, Siberian Federal University, 95 Ave. Prospekt im. Gazety "Krasnoyarskiy Rabochiy", 660025 Krasnoyarsk, Russia; g.shvedov@mail.ru
4 Russian Platinum LLC, Sivtsev Vrahzek Side-Street, 39, 119002 Moscow, Russia; polonyankin@russian-platinum.ru
* Correspondence: tolst@igm.nsc.ru

Received: 30 June 2020; Accepted: 30 July 2020; Published: 31 July 2020

Abstract: The purpose of this study is to show the patterns of distribution of disseminated sulfide in layered rocks based on the numerous geochemical and mineralogical data obtained for eight boreholes of the Norilsk intrusion (southern part of the Norilsk 1 deposit). There is a common trend of sulfide liquid fractionation in the Main Ore Horizon, which is composed of picritic and taxite (or olivine) gabbro-dolerites: the Ni/Cu in both rock types decreases down all sections, indicating an increase in the degree of fractionation of the sulfide liquid from top to bottom. On the contrary, the Ni/Fe ratios in pentlandite increase in this direction due to an increase in sulfur fugacity. However, picrite and taxite/olivine gabbro-dolerites are very distinctly separated by Ni/Cu values: these values are >1 in picritic gabbro-dolerite while they are always <1 in taxite/olivine gabbro-dolerite. These rock types are distinguished by sulfide assemblages. The first includes troilite, Fe-rich pentlandite, chalcopyrite, cubanite, talnahite, bornite and copper (low sulfur association); the second one is composed of monoclinic pyrrhotite, chalcopyrite, Ni-rich pentlandite and pyrite (high sulfur association). A two-stage magma injection with different ore specializations is supposed for picritic and taxite/olivine gabbro-dolerites.

Keywords: Norilsk 1 intrusion; platinum–copper–nickel deposits; disseminated ores; mineralogy and geochemical features

1. Introduction

The platinum–copper–nickel deposits of the Norilsk District are located in the northwestern part of the Siberian platform and are associated with the flood basalt of the Permian–Triassic age [1–3]. The Norilsk 1 deposit is located in the northern part of the cognominal intrusion, confined to the Norilsk–Kharaelyakh Fault in the Norilsk Trough. The Norilsk 1 intrusion intruded into the Carbonian–Permian terrigenous stratum of the Tungusska Series and basalts of the Upper Permian–Lower Triassic age [2]. In previous studies, the focus was on the study of promising massive ores [4–22] or low-sulfide horizons [23–30] which are localized in taxitic gabbroic rocks and leucocratic gabbro of the "Upper gabbro series" [29] of Norilsk deposits. The disseminated ores in the Norilsk deposits are less studied [10,11,31–33]. However, the patterns of distribution of ore elements in differentiated series of different rocks, the composition of disseminated sulfide ores and changes in the modes of occurrence of base and noble metals are also of scientific and promising interest.

The disseminated ore of the Norilsk 1 deposit is hosted predominantly by picritic and taxite gabbro-dolerites of the Main Ore Horizon (MOH) [1,10,34]. The features of sulfide mineralization in each unit have been characterized previously [2]; however, the correlation between the types of the host rocks and the chemical and mineral composition of ores is still relevant [3]. This aspect has been recently highlighted based on the mineralogical and geochemical data for borehole PH-14 of the Norilsk 1 deposit [33].

The Norilsk 1 differentiated intrusion is extended in the northeastern direction. Its structure in the middle part is similar to the structure in the northern part previously described [1,2]. The studied area (southern part of the Norilsk 1 deposit) is located between the Zapolyarniy mine in the north and the Maslovskoye deposit in the south. The new data on the composition of disseminated sulfides in the southern part of the Norilsk 1 deposit have been obtained based on a study of eight boreholes (Figure 1). The purpose of this study is to show the mineralogical and geochemical features of sulfide-disseminated ores in different stratigraphic horizons and to reveal the conditions of their formation.

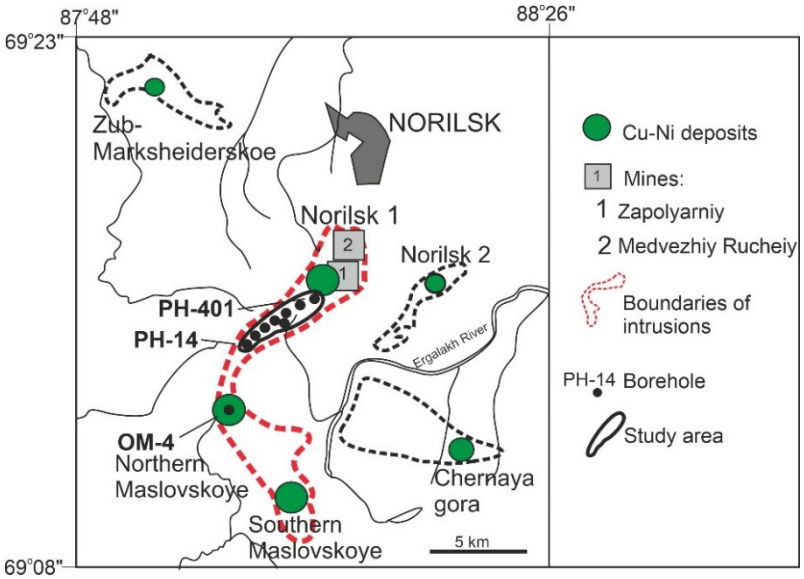

Figure 1. Map of location of ore-bearing intrusions and deposits of the Norilsk District, modified from [3,28].

2. Internal Structure of the Norilsk 1 Intrusion in Its Middle Part

Boreholes intersected the following rocks from top to bottom: tholeiitic basalts of the Nadezhdinsky, Tuklonsky, Khakanchansky, Gudchikhinsky and Syverminsky Suites, rocks of the upper gabbro series (leucogabbro or breccia) with a low-sulfide horizon in PH-72 and PH-222; then main gabbro series (gabbrodiorite, olivine-free, olivine-bearing, olivine and picritic gabbro-dolerite); and rocks of the lower gabbro series (taxite or olivine gabbro-dolerites, and then the contact rocks).

The disseminated sulphide mineralization is found in the low-sulfide horizon as well as picritic, taxite, and olivine (lower) gabbro-dolerites. The low-sulphide horizon differs from the disseminated ores of the layered series by the elevated PGE (ppm)/S (wt.%) ratio, which varies within the range of 5–70 ppm, and relatively low Cu and Ni contents (≤1 wt.% total), which are positively correlated with PGE (up to 60–70 ppm) [29]. Vein-disseminated ores are sometimes localized sometimes in sandstones and siltstones in the southern part of the studied cross-section, and in titanium-augite gabbro–dolerite (a moderately alkaline variety of rock) in the middle part of the cross-section.

The taxite gabbro-dolerite of the lower part of the cross-section, which is so characteristic of the Talnakh intrusion and the Norilsk 1 deposit [28], is present only in three boreholes (PH-72, PH-133, PH-175) as shown in the section along the exploration lines L7 (Figure 2). Olivine gabbro-dolerite is found in the place of taxite gabbro-dolerite in the other boreholes (PH-14, PH-193, PH-222, PH-243, PH-401; sections along exploration lines L1 and L19).

The ratio of rock-forming minerals in olivine gabbro-dolerites from the lower gabbro series is similar to that of the main gabbro series: 50% plagioclase, 30% clinopyroxene, 5% orthopyroxene and 15% olivine [10]. However, the upper olivine gabbro-dolerites are barren, while the lower ones contain sulfide mineralization (disseminated ores).

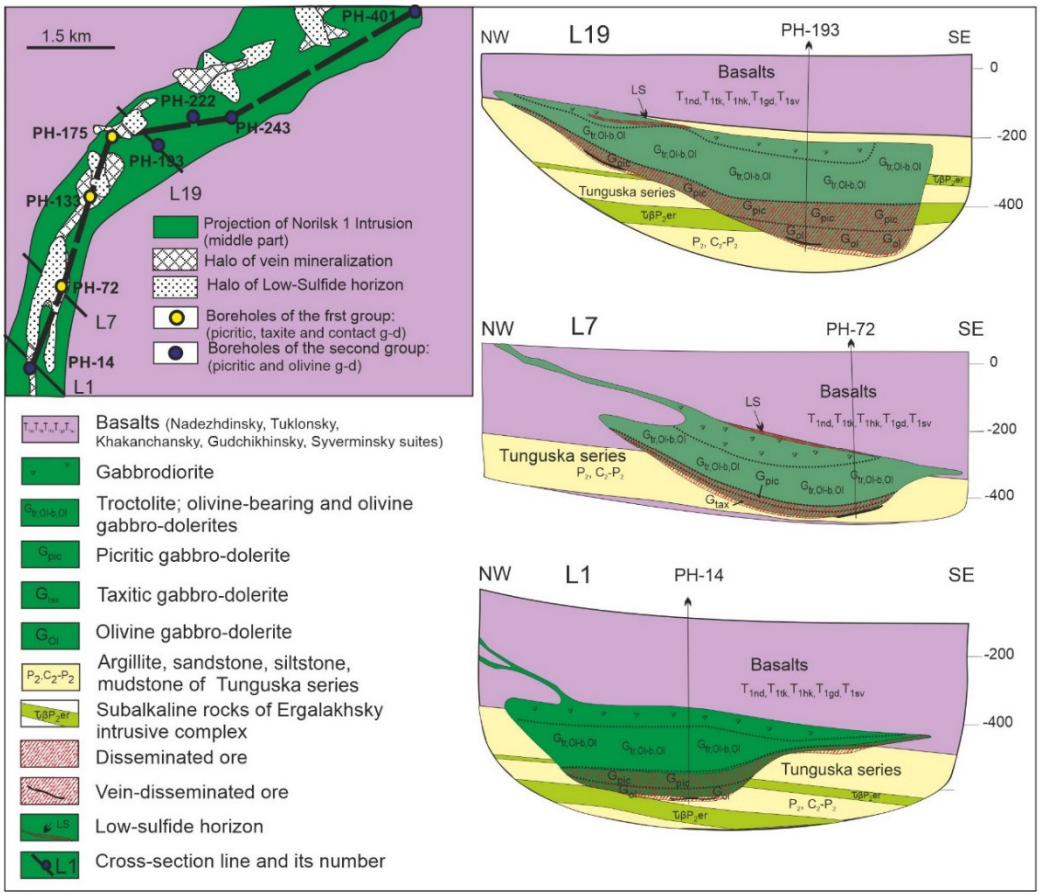

Figure 2. Location of boreholes within the study area (the middle part of the Norilsk 1 intrusion) according to Novageo LLC, and cross-sections along the exploration lines.

3. Methods

The samples were collected from the cores of the exploration boreholes. We conducted the rock analyses for Pd, Pt, Au, Cu, Ni, Co, and S performed in the laboratory of the Stewart Geochemical and Assay LLS, Moscow using the inductively coupled plasma atomic emission spectrometry (ICP-AES) by assay analysis after dissolution in a mixture of acids (codes ME-ICP61 and PGM-ICP23). The Method is sensitive for Au, Pd—0.01–10 ppm, Pt—0.05–10 ppm; Co, Ni, Cu—1–10,000 ppm, S—0.01–10%.

In addition, about 80 combined samples of various compositions of gabbro-dolerites were analyzed for all PGE (including Os, Ir, Ru) in the Testing and Analitical Center for quantitative chemical analyses of Gipronickel Institute LLC using the method of inductively coupled plasma mass spectrometry (ICP-MS), with a preliminary content of these elements on nickel matte. A sample of matte is dissolved in hydrochloric acid, and nitric acid is added to the solution. In this case, the insoluble precipitate is additionally dissolved with moderate heating. The content of noble metals is measured in the solution. The "iCAP-Qc" from the Thermo Fisher Scientific corporation and atomic absorption spectrometry ("iCE 3000 Series") with a reaction-collision cell are used to suppress spectral overlaps to eliminate polyatomic overlaps from matrix elements (Cu, Ni).

Numerous (about 1000) EDS analyses were performed in the Norilsk Nickel R&D Center in the Siberian Federal University on a Tescan Vega 3 SBH instrument (Oxford X-Act EMF analyzer), Krasnoyarsk. The probe size was 270 nm, the accelerating voltage 20 kV.

The wavelength dispersion spectrometry (WDS) analyses of sulfides for testing the EDS data were performed with a JEOL JXA-8100 electron microprobe in the Analytical Center of Multi-Elemental and Isotope Research of the VS Sobolev IGM of the SB RAS, Novosibirsk (Karmanov Head). The accelerating voltage is 20 kV; the probe current is 30–50 nA over the surface of the specimen for both sulfides and PGM; the probe diameter is ~1 μm. The duration of measurement is 20 s for each analytical line. The overlapping of elements in the X-ray spectra was evaluated using the OVERLAP CORRECTION software. Analytical conditions are shown in Table 1. The contents of elements were calculated with the XPP program for the microprobe software. The accuracy and reproducibility of the analytical procedures were evaluated with special tests [35].

Table 1. Analytical conditions for determining the composition of minerals.

Analytical Line	Crystal	Standard	BG− mm	BG+ Mm	Detection Limit, wt.%	Interference
S Kα	PET	$CuFeS_2$	0.0	1.5	0.01	Pt
Fe Kα	LIF	$CuFeS_2$	2.2	2.15	0.02	–
Co Kα	LIF	Fe-Co-Ni alloy	0.6	0.6	0.02	Fe
Ni Kα	LIF	Fe-Co-Ni alloy	1.25	1.25	0.02	–
Cu Kα	LIF	$CuFeS_2$	1.3	1.5	0.02	–
As Lα	TAP	FeAsS	1.5	1.5	0.04	–

Background from right (BG+) and left (BG−) sides of analytical line. Detection limit calculated for 1σ-criteria. Interference—elements with lines overlapping the analytical signal.

4. Results

4.1. Variations in Ore Elements in the Cross-Sections of Intrusion

4.1.1. PH-14

A schematic column for the interval of the Main Ore Horizon in borehole PH-14 is shown in Figure 3. This interval includes the picritic and taxite gabbro-dolerites, vein-disseminated ores in the lower part of the section, and sedimentary rocks. A 36-m thick chromite horizon has been identified in the picritic gabbro-dolerites on the basis of abundant chromian spinel (CrCp). The chromite horizon is delineated from the finding of chromian spinel in polished samples (in reflected light). Cr-Sp occurs as a dissemination of small isometric grains, which are included in both silicate minerals and sulfides. Cr-Sp grains are unevenly distributed in the chromite horizon: from single grains among sulfides to dense dissemination, when chromite makes up 3 vol %. The compositions of chromites in the picrite gabbro-dolerite vary very widely [30]. They are confined to the lower part of picritic gabbro-dolerite and are in contact with olivine gabbro-dolerite. Nickel prevails over copper over almost the entire range of picritic gabbro-dolerites: the average Ni/Cu value is 1.24. Positive anomalies of Pt and Pd are observed in the chromite horizon, where a predominance of copper over nickel is observed (Figure 3a).

The opposite pattern is observed in olivine gabbro-dolerite: copper prevails over nickel: the average Ni/Cu value is 0.69. The levels in which Ni/Cu > 1 are also present in these rocks, which coincide with vein-disseminated ores containing a high content of Pd (up to 6.5 ppm), Pt (up to 4 ppm), and S (15 wt.%) (Figure 3a). The Ni/Cu ratios decrease with depth in general. Palladium prevails over platinum in the entire range of picritic and olivine gabbro-dolerites. The ratio of Pd/Pt as a whole increase downward along the cross-section: Pd/Pt = 2.5 (on average) in the upper part of picritic gabbro-dolerite (with CrSp), 2.8 in the lower part, 3.0 in olivine gabbro-dolerite, and 4.4 in vein-disseminated ores [33]. Vein-disseminated ores are phenocrysts of sulfides and their accumulations (schlieres) appear in irregular shape up to 50 mm in size, which make up between 5% and 60% of the

rock volume. Sometimes, there are veins of massive ores 20-cm thick. The cross-section of the PH-14 borehole is similar to the northern intrusive body (OM-4) of the Maslovsky deposit (Figure 1) [3].

4.1.2. PH-72

The schematic column for borehole PH-72 includes taxite rocks of the upper gabbro series, olivine, picritic, taxite, contact gabbro-dolerites, and vein-disseminated ore in titanium-augite basalt (basalt of of moderate alkalinity). The analysis of ore elements and sulfur is shown in Table 2 as an example. The low-sulfide horizon is observed in the upper gabbro series at a depth of 609.7–612.1 m. It is characterized by low contents of Cu (up to 0.10 wt.%), Ni (up to 0.08 wt.%) and S (up to 0.44 wt.%), and elevated contents of PGE (Pd + Pt up to 8.19 ppm). Pd prevails over Pt, and Cu over Ni in this horizon (Figure 3b).

The Ni/Cu ratios gradually decrease down the section from olivine (2.87 on average) to picritic (1.08), to taxite (0.66), then to contact gabbro–dolerites (0.48), again increasing slightly in exocontact ores (0.66) (Figure 3b). The Pd/Pt ratios, on the contrary, increase in this direction from 2.08 (average) in olivine gabbro-dolerite to 2.69 in the exocontact ore. The relatively high contents of PGM (Pd + Pt is 2–8 ppm) have been noted in the chromite horizon, which was identified at the bottom of picritic gabbro-dolerite. Contents of Pd and Pt increase in taxite gabbro-dolerite, reaching 7.69 ppm and 3.12 ppm, respectively. These contents are even higher in the ores: Pd is 10 ppm, and Pt is 3.5 ppm (Figure 3b).

4.1.3. PH-133

The schematic column for borehole PH-133 includes picritic and taxite gabbro-dolerites, a thin horizon of densely disseminated ores in the lower part of taxite gabbro dolerites, mudstone and Ti-augite dolerites (Figure 3c). A chromite horizon with a thickness of more than 60 m has been identified in picritic gabbro-dolerites. It is confined to the lower part of the picritic gabbro–dolerites. Nickel prevails over copper in almost the entire range of picritic gabbro-dolerites (Figure 3c): the average value of Ni/Cu is 1.24. In this interval, there are several points with a predominance of copper over nickel, which coincide with the Pt-Pd anomalies. Down the picritic gabbro-dolerite section, the Ni/Cu ratios decrease and, finally, they become less than one near the contact with taxitie gabbro-dolerite, in which the average Ni/Cu value is 0.61. Palladium prevails over platinum over the entire interval of rocks of borehole PH-133. The Ni/Cu and Pd/Pt ratios correlate negatively in picritic gabbro-dolerite (the palladium content increases with a decrease in the nickel content), while such a regularity does not occur in taxite, contact gabbro-dolerites and mudstones (Figure 3c).

4.1.4. PH-193

Olivine gabbro-dolerite (main gabbro series) of borehole PH-193 has low contents of all ore elements (Cu does not exceed 0.01, Ni 0.07 wt.%, Pt + Pd—0.03 ppm). The ratios of Ni/Cu are 6–7. The content of Ni reaches 0.34 wt.%, Cu 0.40 wt.%, and Pt + Pd 3.05 in picritic gabbro-dolerite. In general, nickel prevails above copper: the Ni/Cu ratio is 2.6 (average). The chromite horizon was not intersected in the picritic gabbro–dolerite of borehole PH-193 (Figure 3e). Copper (up to 0.32 wt.%) prevails over nickel (up to 0.22 wt.%) in the lower olivine gabbro-dolerite: the Ni/Cu ratios are 0.58 on average. The total content of Pd + Pt reaches 3.13 ppm. The vein-disseminated ore with a thickness of about 10 m is located at the contact with sandstone. The content of Cu reaches 3.19, and Ni 1.04 (wt.%), and Ni/Cu is 0.5 on overage, Pd + Pt—20.0 ppm (Figure 3e). The Pd/Pt ratios vary significantly in the olivine gabbro-dolerite, but, in general, they increase down the section, while the values of Ni/Cu decrease smoothly.

4.1.5. PH-222

A schematic column for borehole PH-222 is shown in Figure 3f. It includes two intervals: the first interval is composed of feldspar and labrador basalts and breccias with a low-sulfide horizon; the second

interval includes picritic, olivine, contact and titanium-augite gabbro-dolerites with a horizon of vein mineralization. Nickel prevails over copper only in the low-sulfide horizon of the upper gabbro series and in picritic gabbro-dolerites (Ni/Cu is 1.35), intensively decreasing down the section; the Ni/Cu ratios are less than 1 in olivine, contact and in Ti-augite gabbro-dolerites (0.54, 0.63 and 0.17, respectively). Palladium significantly prevails over platinum in picritic, olivine gabbro-dolerites and in vein ore (the Pd/Pt ratios are 3.16, 2.79 and 2.63, respectively), while the content of Pt prevails over Pd in basalts, contact and Ti-augite gabbro-dolerites, where the absolute contents of noble metals are very low. The amounts of Pt and Pd reach almost 9 ppm in the vein ore. The contents of Pd + Pt and S in disseminated ores hosted in picritic and olivine gabbro-dolerites show a positive correlation.

4.1.6. PH-243

A column for borehole PH-243 includes picritic, olivine and contact gabbro-dolerites (Figure 3g). A 12.8-m thick chromite horizon located in the middle part of picritic gabbro-dolerite has been distinguished. Nickel prevails over copper in picritic gabbro-dolerite; the average value of Ni/Cu is 1.40, but, in the chromite horizon, copper prevails over nickel (Ni/Cu is 0.81 on average). The PGE anomalies are confined to the chromite horizon (Pd + Pt in total reaching 5 ppm) and the bottoms of picritic gabbro-dolerites. The chromite horizon divides the picritic gabbro-dolerite into two rhythms, in each of which the Cu contents increase down the section. Copper prevails over nickel in olivine gabbro-dolerite: the average value of Ni/Cu is 0.68. Palladium prevails over platinum throughout the studied section. The Pd/Pt value varies from 2 to 4 (2.28 on average) in picritic gabbro-dolerite, gradually increasing down the section, and varies significantly from 1 to 7 (average 2.65) in olivine gabbro-dolerite.

4.1.7. PH-401

The schematic column for borehole PH-401 (Figure 3h) includes two intervals of olivine gabbro-dolerite (main and lower gabbro series) and picritic gabbro-dolerite. A chromite horizon with a thickness of about 22 m is distinguished in the middle part of picritic gabbro-dolerite. The high contents of all ore elements coincide with this horizon, where sulfide schlieres are noted: Pd up to 10 ppm, Pt up to 6 ppm, Ni up to 3.26 wt.% and Cu up to 5.96 wt.%. High sulfur contents (15 wt.%) coincide with the same anomalies (Figure 3h). Palladium prevails over platinum in almost the entire section, with the exception of single horizons with sulfide schlieres. The Ni/Cu ratios reach their maximum values in the upper olivine gabbro-dolerite and decrease down the section, while the Pd/Pt ratios, on the contrary, increase down the section. The content of palladium increases with the increase in copper. The upper olivine gabbro-dolerite of the main layered series is geochemically different from the lower layer of olivine gabbro-dolerite of the MOH: the average value of Ni/Cu is 5.1 and of Pd/Pt 1.52 in the first case, and Ni/Cu is 0.78 and Pd/Pt is 3.09 in the second case.

4.2. Mineralogy and Geochemical Features of Sulphide Mineralization in Various Types of Rocks

A low-sulfide horizon (borehole PH-72, 607–613 m) is located in the gabbro series at the top of the intrusion (Figure 3b). The contents of Cu and Ni are insignificant (0.06–0.18 wt.% in total), while Pd and Pt in total reach 9 ppm in the low-sulfide horizon. Monoclinic pyrrhotite is characteristic of this horizon: $Fe_{0.92}Ni_{0.01}S_{1.08}$ (Table 3). Pentlandite is nickel rich and constantly contains up to 5.48 wt.% of Co: $(Fe_{3.66}Ni_{4.59}Co_{0.73})_{8.98}S_{8.02}$. Sperrylite, ferrous platinum, and As-bearing atokite were found in the low-sulfide horizon of borehole PH-72.

Olivine and olivine-bearing gabbro-dolerite of the main layered series (boreholes PH-72, PH-175, PH-193, PH-401) contain the lowest contents of ore elements (Cu, Ni), not exceeding 0.2 wt.%. These rocks are characterized by the highest Ni/Cu ratios (1.5–9) and the lowest Pd/Pt ratios (0.9–2.2) in comparison with the rock of the other stratigraphic varieties (Figure 3b,d,e,h). Oxides (titanomagnetite, ilmenite) prevail in the ore association of these rocks. Moreover, sulfides (pyrite, chalcopyrite) do not exceed 1–2%, or are represented by single grains. Pyrrhotite is close to troilite $Fe_{0.97}S_{1.03}$ and pentlandite is Fe

rich $(Fe_{5.27}Ni_{3.53}Co_{0.12})_{8.92}S_{8.08}$ in olivine gabbro-dolerite (Table 3). The PGMs include kotulskite Pd (Te, Bi) and mertieite II Pd_8Sb_3.

Picritic gabbro-dolerite is located below the olivine gabbro-dolerite and is characterized by variable thickness (from13 m in PH-72 to 70 m in PH-133) (Figure 3). This rock is observed in all cross-sections. The contents of ore elements as a rule does not exceed: Cu 0.7 wt.%, Ni 0.5 wt.%, Pd 5 ppm and Pt 2 ppm. However, the ore anomalies are observed within the chromite horizons: Cu—6 wt.%, Ni—2 wt.%, Pd and Pt up to 10 ppm (Figure 3h). In almost all the intervals of picritic gabbro-dolerite, the content of nickel prevails over copper (the average value of Ni/Cu is 1.24 in PH-14). An intensive decrease in the Ni/Cu ratios occurs in the upper horizons of picritic gabbro-dolerites; then, these ratios gradually decrease in the lower contact of these rocks (Figure 3c–f). In turn, the Pd/Pt ratios, on the contrary, increase down the cross-sections. The picritic gabbro-dolerite is divided by a chromite horizon into two geochemical rhythms in some cases, in each of which these trends are repeated. This is mostly evident in borehole PH-243 (Figure 3g). The droplet-like, irregular and interstitial sulfide aggregates up to 5 mm are characteristic of picritic gabbro-dolerite (Figure 4a–e). A variable ratio of pyrrhotite, chalcopyrite, pentlandite, cubanite, talnakhite (mooihoekite), bornite, chalcocite, native copper (Figure 4f), chromian spinel, magnetite and ilmenite have been found. Sphalerite, galena, native gold and PGM are included in this assemblage in minor amounts.

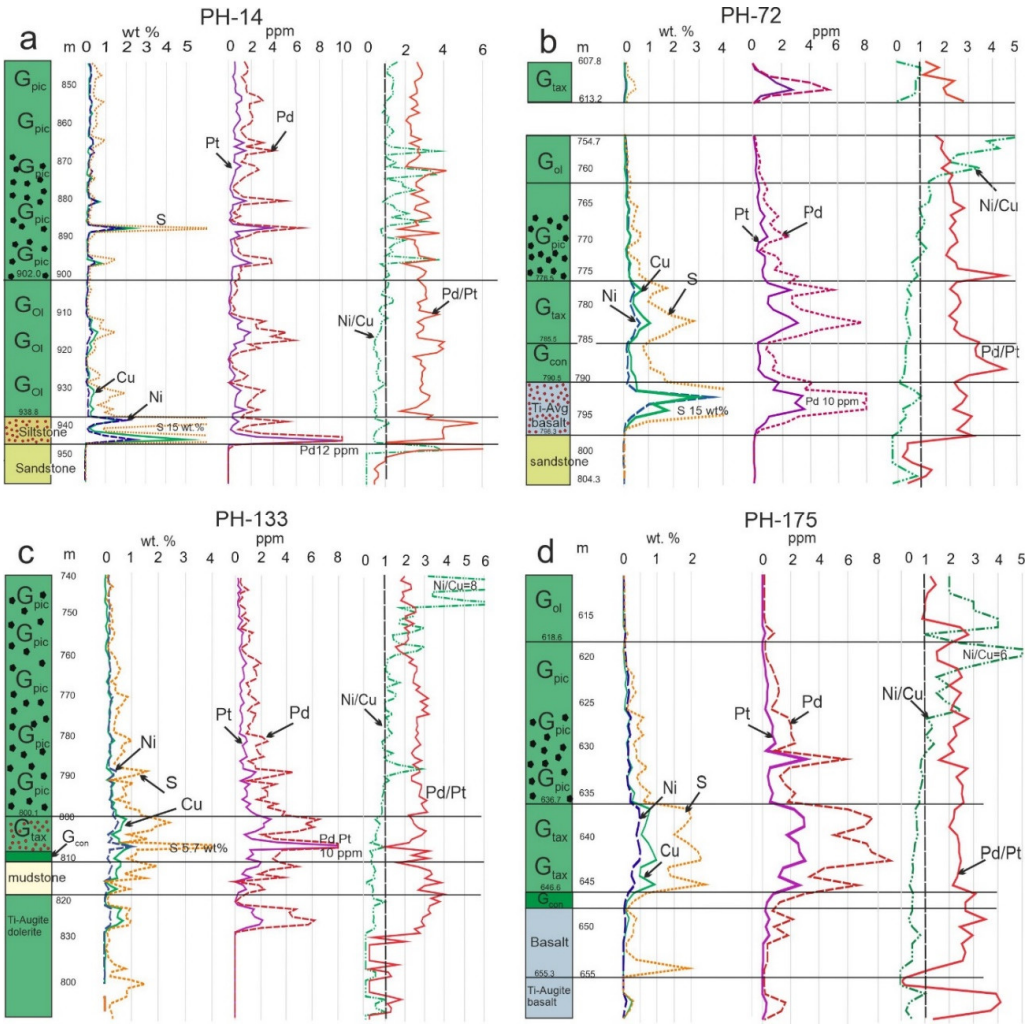

Figure 3. *Cont.*

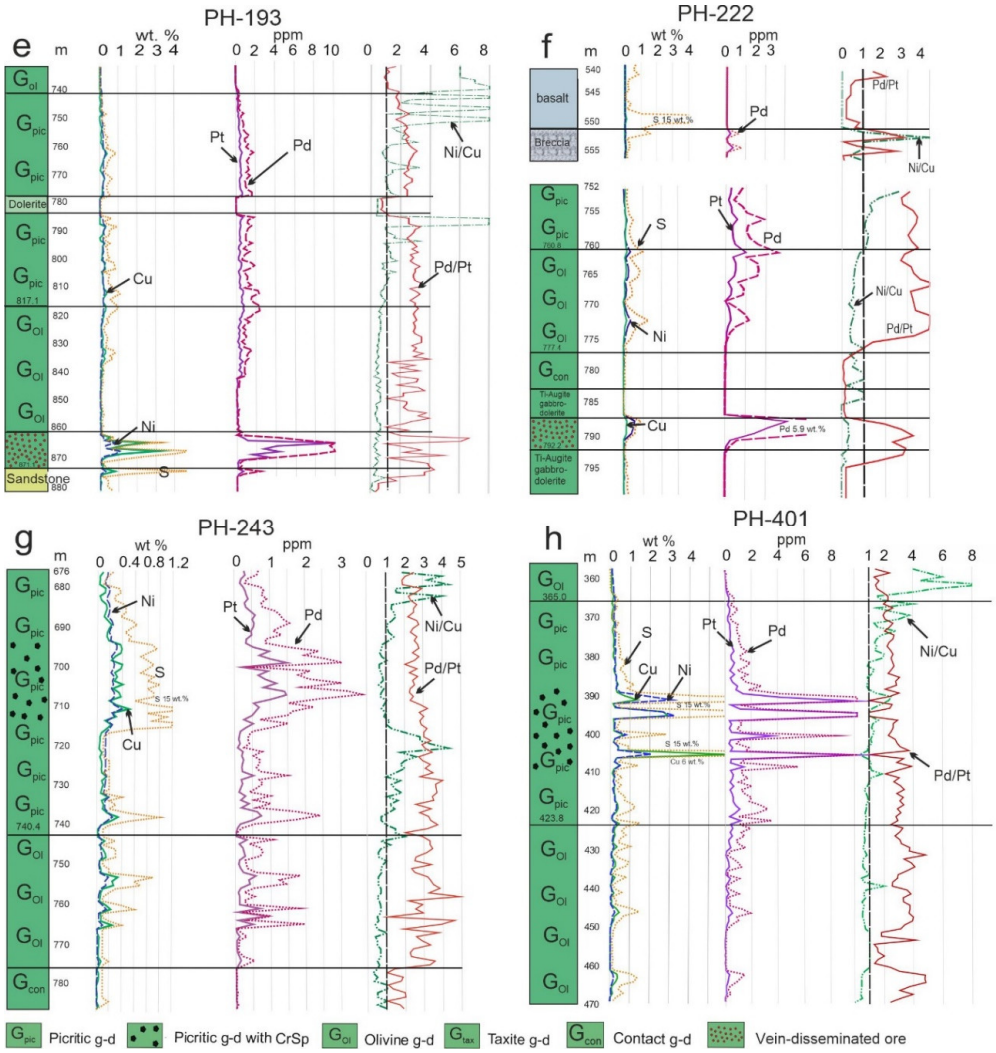

Figure 3. Variations in the contents of ore elements and sulfur in rocks along the cross-section of boreholes; boreholes: (**a**) PH 14, (**b**) PH-72, (**c**) PH-133, (**d**) PH-175, (**e**) PH-193, (**f**) PH-222, (**g**) PH-243, (**h**) PH-401; g–d—gabbro-dolerite, CrSp—chromian spinel. All the names of rocks are given according to the classification adopted by production geologists in the description of the Norilsk deposits, and according to Novageo LLC. "Ti-Augite" suggests that the rock belongs to the moderately alkaline series.

Table 2. Contents of ore elements and S in the rocks of borehole PH-72.

Depth, m	Cu	Ni	Co	S	Pt	Pd	Au
			wt.%			ppm	
Taxite rocks with low-sulfide horizon							
610.5	0.03	0.03		0.12	1.09	1.20	0.03
611.3	0.09	0.07	0.01	0.39	1.68	4.03	0.10
612.1	0.10	0.08	0.01	0.44	2.79	5.40	0.14
613.2	0.04	0.03		0.14	0.59	1.21	0.04
Olivine gabbro dolerite							
758.7	0.05	0.12	0.01	0.15	0.22	0.49	0.02
759.7	0.03	0.11	0.01	0.10	0.19	0.36	0.02
760.7	0.07	0.14	0.01	0.20	0.25	0.58	0.02
761.7	0.09	0.14	0.01	0.26	0.36	0.78	0.03
762.7	0.09	0.14	0.01	0.23	0.43	0.98	0.04
763.6	0.08	0.13	0.01	0.19	0.29	0.67	0.03
764.5	0.09	0.14	0.01	0.20	0.37	0.87	0.04

Table 2. *Cont.*

Depth, m	Cu	Ni	Co	S	Pt	Pd	Au
	wt.%				ppm		
Picritic gabbro-dolerite							
765.5	0.19	0.22	0.01	0.54	0.48	1.35	0.06
766.5	0.14	0.17	0.01	0.42	0.79	1.77	0.06
767.5	0.13	0.18	0.01	0.39	0.49	1.20	0.05
768.5	0.12	0.15	0.01	0.30	0.68	1.49	0.05
769.5	0.25	0.25	0.01	0.70	1.00	2.40	0.10
771.5	0.07	0.10	0.01	0.18	0.24	0.52	0.02
772.5	0.10	0.12	0.01	0.19	0.80	1.62	0.05
773.5	0.25	0.21	0.01	0.60	0.81	1.98	0.08
774.5	0.20	0.18	0.01	0.60	0.59	1.47	0.06
775.5	0.22	0.24	0.01	0.60	0.70	3.14	0.08
776.5	0.37	0.29	0.01	0.95	1.03	2.56	0.12
Taxite gabbro-dolerite							
777.5	0.71	0.46	0.02	1.70	2.59	5.66	0.25
778.5	0.40	0.31	0.01	1.12	1.09	2.74	0.11
779.5	0.37	0.24	0.01	0.98	1.03	2.72	0.12
780.5	0.53	0.34	0.01	1.38	1.37	3.38	0.18
781.5	0.77	0.44	0.01	1.85	2.50	5.39	0.30
782.5	1.03	0.63	0.02	2.76	3.12	7.69	0.38
783.5	0.61	0.44	0.01	2.03	1.96	4.64	0.24
784.5	0.50	0.37	0.01	1.69	1.19	3.14	0.15
785.5	0.20	0.12	0.01	0.98	0.31	1.05	0.05
Contact gabbro-dolerite							
786.5	0.18	0.10	0.01	0.76	0.27	0.86	0.05
787.5	0.29	0.16	0.01	0.92	0.43	1.41	0.07
788.5	0.28	0.16	0.01	1.08	0.43	1.58	0.09
789.5	0.28	0.14	0.01	1.08	0.28	1.25	0.06
Vein-disseminated ore in Ti-augite basalt							
790.5	0.44	0.20	0.01	1.61	0.75	2.23	0.13
791.5	0.51	0.14	0.01	1.66	1.76	4.14	0.26
792.2	0.54	0.48	0.02	4.03	1.39	3.57	0.13
792.4	2.92	3.44	0.11	15.00	3.46	10.00	0.34
793.3	1.18	1.01	0.04	7.68	2.92	7.85	0.38
794.3	1.73	0.67	0.03	5.98	3.59	8.35	0.63
795.3	0.48	0.29	0.01	3.79	1.04	3.20	0.15
796.3	0.22	0.07	0.01	0.97	0.81	2.28	0.10
797.3	0.05	0.02		0.09	0.17	0.42	0.02
Sandstone							
798.3		0.01		0.01	0.01	0.03	0.01
799.3	0.01			0.01	0.01	0.00	0.01

Note. Empty cell—below detection limit.

Magnetite is common there (Figure 4a), the amount of which is negatively correlated with the amount of chromian spinel in the chromite horizons of these rocks and with ilmenite in the lower horizons of picritic gabbro-dolerite. Pyrrhotite is most common in the upper horizons of picritic gabbro-dolerite (Figure 4b). The amounts of pyrrhotite and pentlandite decrease with depth. Cubanite and chalcopyrite in the sulfide aggregates begin to dominate lower in the profile of the picritic gabbro-dolerite (Figure 4e). Chromian spinel is common at certain stratigraphic levels (chromite horizons) of picritic gabbro-dolerite (Figure 4a). The Cu-rich sulfides (talnakhite, bornite, chalcocite) and native copper are subordinate, but they are a typomorphic feature of the sulfide association (Figure 4c,f) in picritic gabbro-dolerite and are not characteristic of other rocks. A variety of copper-rich minerals from picritic gabbro-dolerite (PH-14) are shown in [33]. The composition of

pyrrhotite is close to troilite ($Fe_{1.00}S_{1.00}$); pentlandite is Fe rich ($(Fe_{5.21}Ni_{3.64}Co_{0.11})_{8.96}S_{8.04}$) in most picritic samples of all boreholes (Figure 5a,b; Table 3). The content of Fe predominates slightly over Cu in chalcopyrite; in this case, chalcopyrite occurs often as an exsolution texture with cubanite. When the chalcopyrite becomes less ferruginous, cubanite is not detected in the association. Pyrrhotite is gradually enriched with sulfur, and pentlandite is enriched with nickel down the borehole section.

The largest number of PGM grains is found in chromite horizons, consistent with the highest contents of Pd and Pt, which have a sawtooth distribution. PGMs are represented by numerous compounds: paolovite, atokite, rustenburgite, mayakite, menshikovite, polarite, sperrylite, tetraferroplatinum, sobolevskite, hollingworthite and kotulskite. These compounds do not exhibit common patterns in their distribution over the depth of the interval of picritic gabbro-dolerites. Native gold and Au-Ag alloys are characteristic of the lower parts of the picritic gabbro-dolerite section.

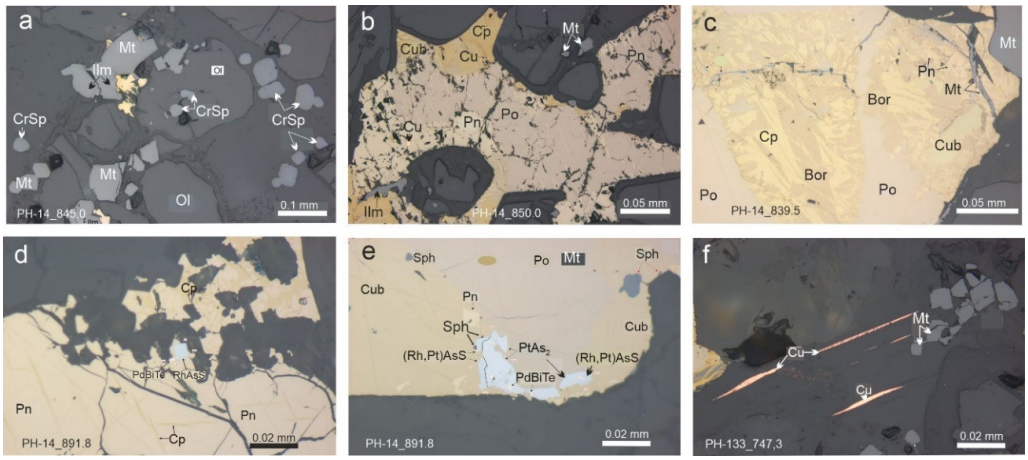

Figure 4. Microparageneses of the minerals in the picritic gabbro-dolerite: (**a**) PH-14_845.0; (**b**) PH-14_850.0; (**c**) PH-14_839.5; (**d**,**e**) PH-14_891.8; (**f**) PH-133_747.3. Abbreviation (hereinafter): Ilm—ilmenite, Mt—magnetite, CrSp—chromian spinel, Ol—olivine, Cub—cubanite, Po—pyrrhotite, Pn—pentlandite, Cu—native copper, Sph—sphalerite, Bor—bornite, Cp—chalcopyrite.

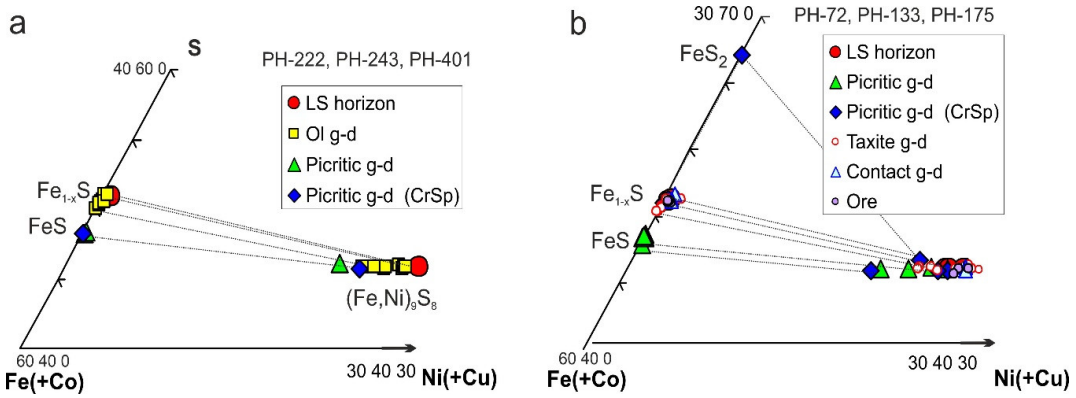

Figure 5. Composition of sulfides in the Fe(+Co) – Ni–S system: (**a**) boreholes in which the lower layered series is represented by olivine gabbro-dolerites; (**b**) boreholes in which the lower layered series is represented by taxite gabbro-dolerites.

Taxite gabbro-dolerite located below the picritic gabbro-dolerite is about 10-m thick in all the studied boreholes (Figure 3b–d). The content of copper (up to 1.0 wt.%) prevails over nickel (up to 0.8 wt.%) throughout the sections of taxite gabbro-dolerite (PH-72, PH-133, PH-175); the Ni/Cu ratios are less than one (e.g., 0.57 on average in borehole PH-133), and they decrease down the cross-sections. The palladium content (2–10 ppm) prevails over platinum (0.8–3 ppm); the Pd/Pt ratios vary significantly throughout the range of taxite gabbro-dolerite.

Table 3. Sulfide compositions in the Main Ore Horizon of the Norilsk 1 intrusion.

No	Comment	Depth	Rock	S	As	Cu	Fe	Ni	Co	Pd	Total
1	PH-133 Cp	771.6	Picritic g-d	35.07	0.03	34.21	30.27	0.10	0.00	0.00	99.68
2	PH-133 Pn	771.6	Picritic g-d	33.32	0.00	0.70	31.92	32.34	1.16	0.00	99.44
3	PH-133 Po	771.6	Picritic g-d	36.36	0.00	0.28	62.77	0.07	0.00	0.00	99.47
4	PH-133 Pn	786.7	Picritic g-d	33.06	0.00	0.05	30.00	34.63	1.32	0.00	99.06
5	PH-133 Pn	798.4	Picritic g-d	32.98	0.00	0.00	34.44	30.49	0.87	0.00	98.78
6	PH-133 Po	798.4	Picritic g-d	36.48	0.00	0.00	62.97	0.00	0.00	0.00	99.46
7	PH-133 Cp	804.4	Taxite g-d	34.99	0.00	34.85	30.33	0.00	0.00	0.00	100.17
8	PH-133 Pn	804.4	Taxite g-d	32.99	0.00	0.00	27.19	38.26	0.61	0.07	99.13
9	PH-133 Po	804.4	Taxite g-d	39.46	0.00	0.00	57.84	1.99	0.00	0.00	99.29
10	PH-133 Cp	810.7	Taxite g-d	35.01	0.00	34.59	30.05	0.00	0.00	0.00	99.65
11	PH-133 Pn	810.7	Taxite g-d	33.27	0.05	0.00	30.00	35.81	0.62	0.06	99.80
12	PH-133 Po	810.7	Taxite g-d	39.44	0.00	0.07	59.24	0.36	0.00	0.00	99.11
13	PH-133 Cp	811.1	Contact g-d	35.01	0.00	34.70	30.24	0.00	0.00	0.00	99.95
14	PH-133 Pn	811.1	Contact g-d	33.25	0.00	0.00	29.05	36.46	0.99	0.00	99.75
15	PH-133 Po	811.1	Contact g-d	39.55	0.00	0.08	59.06	0.77	0.00	0.00	99.46
16	PH-133 Cp	811.9	Contact g-d	34.98	0.00	34.57	30.12	0.05	0.00	0.00	99.72
17	PH-133 Pn	811.9	Contact g-d	33.35	0.00	0.00	28.40	36.74	1.31	0.04	99.83
18	PH-133 Po	811.9	Contact g-d	39.44	0.00	0.00	58.68	0.98	0.00	0.00	99.09
19	PH-243 Cp	695.2	Picritic g-d	35.00	0.00	34.57	30.74	0.03	0.00	0.00	100.35
20	PH-243 Po	695.2	Picritic g-d	36.45	0.00	0.24	63.59	0.00	0.00	0.00	100.28
21	PH-243 Cp	700.3	Picritic g-d	34.95	0.00	34.16	30.72	0.15	0.00	0.00	99.98
22	PH-243 Pn	700.3	Picritic g-d	33.34	0.05	0.84	37.16	27.35	0.76	0.00	99.51
23	PH-243 Po	700.3	Picritic g-d	36.47	0.00	0.22	63.00	0.00	0.00	0.00	99.68
24	PH-243 Po	725.6	Picritic g-d	36.41	0.00	0.10	63.56	0.00	0.00	0.00	100.09
25	PH-243 Cp	736.6	Picritic g-d	35.08	0.00	34.51	30.39	0.00	0.00	0.00	99.98
26	PH-243 Pn	736.6	Picritic g-d	33.23	0.00	0.04	35.44	30.58	1.04	0.09	100.42
27	PH-243 Po	736.6	Picritic g-d	36.39	0.03	0.00	63.56	0.00	0.00	0.00	99.98
28	PH-243 Cp	763.8	Olivine g-d	34.93	0.00	34.68	30.29	0.00	0.00	0.00	99.90
29	PH-243 Cp	773.5	Olivine g-d	34.94	0.00	34.49	30.65	0.04	0.00	0.00	100.12
30	PH-243 Pn	773.5	Olivine g-d	33.43	0.00	0.00	31.01	34.80	1.38	0.00	100.62
31	PH-243 Po	773.5	Olivine g-d	39.04	0.00	0.04	60.52	0.23	0.00	0.00	99.83
32	PH-401 Cp	434.9	Olivine g-d	35.21	0.00	34.60	30.16	0.03	0.00	0.00	100.00
33	PH-401 Pn	434.9	Olivine g-d	32.97	0.00	0.00	31.36	34.99	0.60	0.00	99.92
34	PH-401 Po	434.9	Olivine g-d	39.63	0.00	0.00	60.44	0.13	0.00	0.00	100.20
35	PH-401 Cp	439.2	Olivine g-d	34.99	0.00	34.54	30.50	0.00	0.00	0.00	100.03
36	PH-401 Pn	439.2	Olivine g-d	33.14	0.00	0.00	33.92	30.74	2.09	0.00	99.89
37	PH-401 Po	439.2	Olivine g-d	38.49	0.00	0.00	61.75	0.06	0.00	0.00	100.30
38	PH-401 Cp	442.3	Olivine g-d	35.10	0.00	34.87	30.48	0.09	0.00	0.00	100.54
39	PH-401 Pn	442.3	Olivine g-d	33.10	0.00	0.00	32.93	33.09	0.85	0.06	100.03
40	PH-401 Po	442.3	Olivine g-d	38.57	0.05	0.00	61.10	0.25	0.00	0.00	99.97
41	PH-401 Cp	445	Olivine g-d	35.18	0.00	34.87	30.22	0.00	0.00	0.00	100.26
42	PH-401 Pn	445	Olivine g-d	33.12	0.00	0.00	32.81	33.00	0.90	0.00	99.83
43	PH-401 Po	445	Olivine g-d	39.39	0.00	0.00	60.30	0.12	0.00	0.00	99.81
44	PH-401 Cp	447.9	Olivine g-d	35.29	0.00	34.88	30.55	0.05	0.00	0.00	100.78
45	PH-401 Pn	447.9	Olivine g-d	33.18	0.00	0.00	32.93	33.27	0.66	0.00	100.04
46	PH-401 Po	447.9	Olivine g-d	38.99	0.00	0.00	60.82	0.16	0.00	0.00	99.96
47	PH-401 Cp	450.7	Olivine g-d	35.01	0.00	34.57	30.21	0.06	0.00	0.00	99.85
48	PH-401 Pn	450.7	Olivine g-d	33.20	0.00	0.00	33.46	32.05	1.18	0.00	99.89
49	PH-401 Po	450.7	Olivine g-d	38.57	0.00	0.00	60.79	0.18	0.00	0.00	99.55
50	PH-401 Cp	452.7	Olivine g-d	35.07	0.00	34.66	30.37	0.04	0.00	0.00	100.14
51	PH-401 Pn	452.7	Olivine g-d	33.18	0.00	0.36	30.75	34.67	1.09	0.06	100.11
52	PH-401 Po	452.7	Olivine g-d	38.89	0.00	0.09	60.41	0.43	0.00	0.00	99.82
53	PH-401 Cp	460.5	Olivine g-d	35.07	0.00	34.64	30.40	0.00	0.00	0.00	100.11
54	PH-401 Pn	460.5	Olivine g-d	33.07	0.00	0.00	30.80	35.15	0.86	0.05	99.94
55	PH-401 Po	460.5	Olivine g-d	39.32	0.00	0.00	59.70	0.43	0.00	0.00	99.45
56	PH-72 Pn	610.5	LS horizon	32.87	0.00	0.00	26.13	34.43	5.48	0.15	99.06

Table 3. *Cont.*

No	Comment	Depth	Rock	S	As	Cu	Fe	Ni	Co	Pd	Total
57	PH-72 Cp	611.5	LS horizon	34.89	0.00	34.48	30.16	0.00	0.00	0.00	99.53
58	PH-72 Po	611.5	LS horizon	39.28	0.00	0.00	59.35	0.60	0.00	0.00	99.23
59	PH-72 Cp	612.5	LS horizon	34.87	0.00	34.50	30.10	0.00	0.00	0.00	99.48
60	PH-72 Pn	612.5	LS horizon	33.08	0.00	0.00	28.49	36.44	1.31	0.15	99.47
61	PH-72 Po	612.5	LS horizon	39.37	0.00	0.00	58.69	1.00	0.00	0.00	99.05
62	PH-72 Cub	765.8	Picritic g-d	34.76	0.00	27.00	36.92	0.00	0.00	0.00	98.68
63	PH-72 Cub	765.8	Picritic g-d	34.64	0.00	31.28	31.55	1.49	0.00	0.00	98.96
64	PH-72 Po	765.8	Picritic g-d	36.31	0.00	0.02	63.20	0.00	0.00	0.00	99.54
65	PH-72 Cp	767.4	Picritic g-d	34.38	0.05	33.70	29.65	0.84	0.00	0.00	98.61
66	PH-72 Pn	767.4	Picritic g-d	33.04	0.00	0.07	38.03	26.55	1.52	0.00	99.22
67	PH-72 Cp	768.8	Picritic g-d	35.05	0.00	34.64	30.18	0.00	0.00	0.04	99.91
68	PH-72 Pn	768.8	Picritic g-d	33.29	0.00	0.00	31.84	34.03	0.95	0.00	100.11
69	PH-72 Po	768.8	Picritic g-d	39.55	0.00	0.00	59.91	0.19	0.00	0.00	99.65
70	PH-72 Cp	770.5	Picritic g-d	34.86	0.00	34.36	30.17	0.00	0.00	0.00	99.39
71	PH-72 Pn	770.5	Picritic g-d	33.25	0.00	0.00	37.59	27.61	0.84	0.00	99.29
72	PH-72 Po	770.5	Picritic g-d	36.52	0.00	0.00	62.90	0.00	0.00	0.00	99.42
73	PH-72 Cp	772.6	Picritic g-d	35.02	0.00	34.54	30.11	0.00	0.00	0.00	99.67
74	PH-72 Pn	772.6	Picritic g-d	32.93	0.06	0.00	30.84	34.80	0.76	0.00	99.40
75	PH-72 Cub	774.4	Picritic g-d	35.33	0.00	23.63	40.43	0.03	0.00	0.06	99.48
76	PH-72 Pn	774.4	Picritic g-d	33.12	0.00	2.16	31.30	28.76	2.03	0.15	97.52
77	PH-72 Po	774.4	Picritic g-d	39.15	0.00	0.00	59.97	0.17	0.00	0.00	99.29
78	PH-72 Cp	775.5	Picritic g-d	34.93	0.00	34.84	30.10	0.00	0.00	0.00	99.87
79	PH-72 Py	775.5	Picritic g-d	53.26	0.00	0.00	46.63	0.00	0.00	0.00	99.89
80	PH-72 Cp	776.4	Picritic g-d	35.03	0.00	34.48	29.94	0.13	0.00	0.00	99.58
81	PH-72 Pn	776.4	Picritic g-d	33.40	0.00	0.00	28.77	36.91	0.67	0.06	99.81
82	PH-72 Po	776.4	Picritic g-d	39.45	0.00	0.00	59.23	0.66	0.00	0.00	99.34
83	PH-72 Cp	777.3	Taxite g-d	35.10	0.00	34.75	30.07	0.00	0.00	0.00	99.92
84	PH-72 Pn	777.3	Taxite g-d	33.34	0.00	0.38	33.01	31.57	1.35	0.00	99.65
85	PH-72 Po	777.3	Taxite g-d	38.57	0.00	0.08	60.85	0.07	0.00	0.00	99.57
86	PH-72 Cp	778.2	Taxite g-d	35.09	0.00	34.65	30.15	0.00	0.00	0.00	99.89
87	PH-72 Pn	778.2	Taxite g-d	33.38	0.00	0.00	32.43	33.12	0.73	0.00	99.66
88	PH-72 Po	778.2	Taxite g-d	38.85	0.00	0.00	60.20	0.22	0.00	0.00	99.27
89	PH-72 Cp	780.3	Taxite g-d	34.90	0.00	34.45	30.29	0.05	0.00	0.00	99.69
90	PH-72 Pn	780.3	Taxite g-d	33.06	0.00	0.00	31.24	33.86	1.26	0.05	99.47
91	PH-72 Po	780.3	Taxite g-d	38.69	0.00	0.07	59.94	0.26	0.00	0.00	98.96
92	PH-72 Cp	781	Taxite g-d	35.02	0.00	34.52	30.20	0.08	0.00	0.00	99.82
93	PH-72 Pn	781	Taxite g-d	33.23	0.00	0.62	33.33	31.11	1.11	0.00	99.40
94	PH-72 Po	781	Taxite g-d	38.30	0.00	0.00	60.65	0.09	0.00	0.00	99.03
95	PH-72 Cp	782	Taxite g-d	35.15	0.00	35.04	29.94	0.00	0.00	0.00	100.13
96	PH-72 Pn	782	Taxite g-d	33.07	0.00	0.00	28.09	37.34	0.79	0.06	99.35
97	PH-72 Po	782	Taxite g-d	39.47	0.00	0.03	58.79	0.97	0.00	0.00	99.25
98	PH-72 Cp	783.7	Taxite g-d	35.00	0.00	34.60	30.09	0.00	0.00	0.00	99.70
99	PH-72 Pn	783.7	Taxite g-d	33.37	0.00	0.00	28.40	36.97	0.69	0.00	99.43
100	PH-72 Po	783.7	Taxite g-d	39.53	0.00	0.00	58.84	1.31	0.00	0.00	99.68
101	PH-72 Cp	790.4	Contact g-d	35.19	0.00	34.46	30.39	0.00	0.00	0.00	100.04
102	PH-72 Pn	790.4	Contact g-d	33.29	0.00	0.00	28.06	37.18	1.83	0.00	100.36
103	PH-72 Po	790.4	Contact g-d	39.51	0.00	0.00	59.16	1.08	0.00	0.00	99.75
104	PH-72 Cp	791.6	Ore	35.03	0.00	34.52	30.38	0.00	0.00	0.00	99.03
105	PH-72 Pn	791.6	Ore	33.34	0.00	0.00	29.28	36.24	1.63	0.00	100.49
106	PH-72 Po	791.6	Ore	39.44	0.00	0.00	59.55	0.74	0.00	0.00	99.73
107	PH-72 Cp	793.5	Ore	34.99	0.00	34.52	30.40	0.00	0.00	0.00	99.91
108	PH-72 Pn	793.5	Ore	33.42	0.00	0.03	27.67	37.45	1.96	0.00	100.53
109	PH-72 Po	793.5	Ore	39.35	0.00	0.00	59.08	1.13	0.00	0.00	99.56
110	PH-72 Cp	795.3	Ore	35.03	0.00	34.07	30.17	0.26	0.00	0.00	99.53

Table 3. *Cont.*

No	Comment	Depth	Rock	S	As	Cu	Fe	Ni	Co	Pd	Total
111	PH-72 Pn	795.3	Ore	33.28	0.00	0.13	28.34	35.97	2.21	0.00	99.94
112	PH-72 Po	795.3	Ore	39.50	0.00	0.26	59.37	0.58	0.00	0.00	99.71
113	PH-72 Cp	796.1	Ore	35.05	0.00	34.53	30.31	0.00	0.00	0.00	99.89
114	PH-72 Pn	796.1	Ore	32.90	0.00	0.00	29.96	35.82	1.23	0.00	99.91
115	PH-72 Po	796.1	Ore	39.28	0.00	0.22	59.33	0.51	0.00	0.00	99.34

Note. Cp—chalcopyrite, Pn—pentlandite, Po—pyrrhotite, Cub—cubanite, g-d—gabbro-dolerite. Ore—weindessimenated ore with schlieres.

The positive anomalies of all ore elements coincide with each other, and are associated with the localization of vein-disseminated ores (Figure 3b–d). Sulfides are represented by interstitial dissemination and schlieres up to 3 cm with a significant predominance of chalcopyrite over the other sulfides (Figure 6a–c). Pyrrhotite is more S rich (monoclinic $Fe_{0.94}S_{1.06}$) and pentlandite is more Ni rich ($(Fe_{3.80}Ni_{5.09}Co_{0.08})_{8.97}S_{8.03}$) (Table 3) than the same minerals in picritic gabbro-dolerite (Figure 5). A minor amount of Ni up to 1.5 wt.% appears in pyrrhotite, close to the contact with the host rocks. In this case, it is associated with Ni-rich pyrite (up to 5.6 wt.% Ni). Pyrrhotite becomes more sulfurous, and pentlandite is enriched in nickel down the cross-section of taxite gabbro-dolerite. Talnakhite and other Cu-rich minerals are absent there. Ilmenite and titanomagnetite are found as inclusions in silicates and as interstitial grains (dissolution texture of titanomagnetite and ilmenite). PGMs are represented by sperrylite, atokite, rustenburgite, paolovite, sobolevskite, moncheite, insizwaite and numerous unnamed phases. Atokite and rustenburgite contain Au (1.31–8.23 wt.%) and Pb (0.86–7.48 wt.%). The Au-Ag alloys are characterized by a predominance of gold over silver, in contrast to those from picritic gabbro-dolerite.

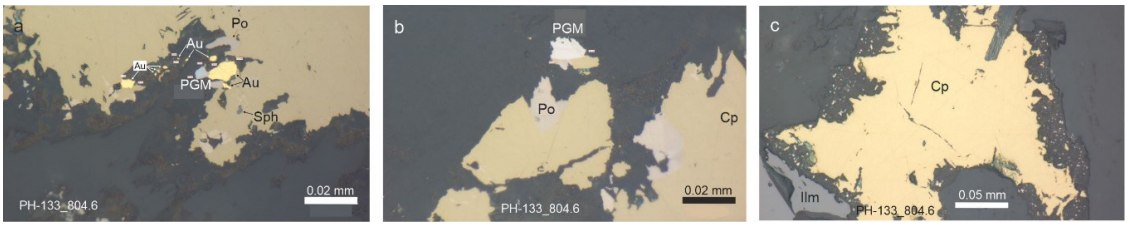

Figure 6. Microparageneses of the minerals in the taxite gabbro-dolerite: (**a**,**b**) chalcopyrite in intergrowth with pyrrhotite (Po), gold (Au) and minerals of platinum group elements (PGM); (**c**) chalcopyrite in intergrowth with ilmenite (Ilm).

Olivine gabbro-dolerite with a variable thickness of 20–50 m is present in the most cross-sections (Figure 3a,e–h). Olivine gabbro-dolerite located below the picritic layer, is similar to taxite gabbro-dolerite and differs from olivine gabbro-dolerite of the main layered series in terms of their geochemical features such as the Ni/Cu ratios are less than one; the variations Cu are 0.3–0.6 wt.%, and Ni 0.2–0.4 wt.% for all boreholes. The contents of PGE show minor anomalies up to 1.8–5.8 ppm for Pd and 0.5–1.4 ppm for Pt. Sulfides are represented by chalcopyrite, pyrrhotite and pentlandite, as well as pyrite, which occurs more often in the lower parts of these interval rocks (Figure 7a–c). Grains of ilmenite and magnetite occur as inclusions in the silicate minerals. Magnetite is also found in a secondary phase. Chromian spinel and Cu-rich sulfide are absent in olivine gabbro-dolerite. A positive correlation between the amounts of chalcopyrite and pentlandite and a negative correlation between both these minerals and the amount of pyrrhotite appear in olivine gabbro-dolerite, which also distinguishes them from picritic ones. Chalcopyrite is predominant in sulfide aggregates at the bottom of this interval (Figure 7c). Sulfides are replaced by pyrite-marcasite-magnetite aggregates and by violarite in some horizons. Pentlandite varies widely in its composition at different horizons from Ni rich ($(Ni_{4.63}Fe_{4.27}Co_{0.11})_{9.01}S_{7.99}$) to Fe rich ($(Fe_{4.54}Ni_{4.35}Co_{0.12})_{9.01}S_{7.99}$) (Table 3), but with a significant

predominance of nickel compounds (Figure 5a). The S content in pyrrhotite and the Ni content in pentlandite increase with depth. Millerite occurs in the association with Ni-rich pentlandite. PGMs are represented by merenskiite, paolovite, naldrettite, menshikovite, etc. Native gold has been identified as fine inclusions in silicates.

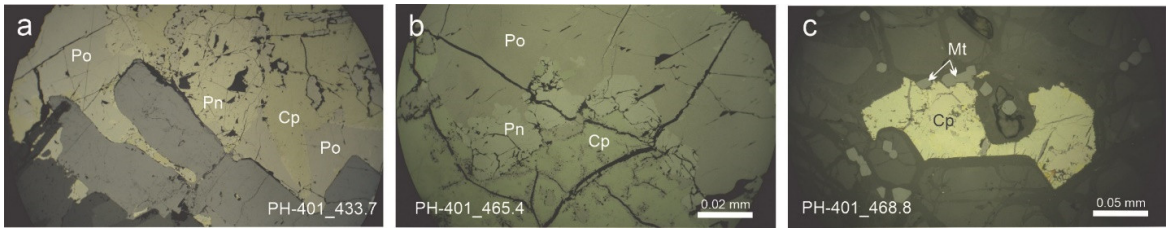

Figure 7. Microparageneses of the minerals in the olivine gabbro-dolerite: (**a**,**b**) pyrrhotite-pentlandite-chalcopyrite aggregates; (**c**) chalcopyrite grain in intergrowth with magnetite (Mt).

Contact gabbro-dolerite is found in most boreholes at the contact of the intrusion with the host rocks in the form of layers 0.3–5-m thick; the greatest thickness of these rocks (up to 10 m) has been identified in boreholes PH-222 and PH-72. Low contents of ore elements (about 5 ppm in PH-72 and PH-133 and less than 1 ppm of PGEs in other boreholes) are observed in contact gabbro-dolerites. These horizons are characterized by schliere-disseminated sulfide mineralizations of pyrrhotite, chalcopyrite and pyrite, as well as of galena in associations with pyrrhotite. According to their mineralogical characteristics, contact gabbro-dolerite is similar to taxite gabbro-dolerites: pyrrhotite is represented by the monoclinic $Fe_{0.91}Ni_{0.01}S_{1.09}$ species, with a minor Ni content of about 1 wt.%. Pentlandite is Ni rich ($(Fe_{3.87}Ni_{4.88}Co_{0.25})_{9.00}S_{8.00}$) (Figure 5b; Table 3). PGMs have not been detected.

Exocontact vein-disseminated ores were intersected by boreholes PH-14 and PH-72, first in siltstones, and then in basalts. These ores differ in their compositions from the disseminated ore of the MOH: pyrrhotite prevails in them (80–85%), while chalcopyrite and pentlandite are about 10–15%. The metal contents in borehole PH-14 reach: Cu 5 wt.%, Ni 3.5 wt.%, Pd 12 ppm, and Pt 10 ppm. Pyrrhotite is represented by large fractured grains with streaks of chalcopyrite and magnetite, and inclusions of pentlandite and sphalerite. The exocontact chalcopyrite-pyrrhotite ore in borehole PH-72 in the horizon about 8-m thick is represented by veinlets and schlieres of sulfides. Interstitial aggregates up to 5 cm are composed of about 40% of the rock volume (Figure 8a–c). The metal contents reach: Cu 2.9 wt.%, Ni 3.4 wt.%, Pd 10 ppm, and Pt 3.5 ppm. Pyrrhotite forms grains up to 5 cm, in which chalcopyrite-pentlandite aggregates and lenticular inclusions of pentlandite are located. Sulfides are surrounded by secondary magnetite. Sperrylite, hollingworthite, palladoarsenide and menshikovite have been found among PGMs.

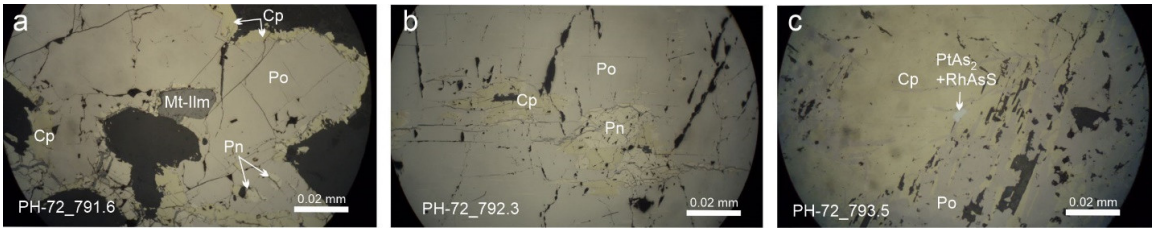

Figure 8. Microparageneses of the minerals in the exocontact vein-disseminated ores: (**a**) pyrrhotite grain in intergrowth with chalcopyrite (Cp), pentlandite (Pn) and magnetite-ilienite- (Mt-Ilm) inclusion; (**b**) pyrrhotite-chalcopyrite-pentlandite grain; (**c**) pyrrhotite-chalcopyrite grain with PGM inclusion ($PtAs_2$+RhAsS).

5. Discussion

5.1. Geochemical Features of Rocks

(1) General patterns of mineralogical-geochemical regularities exist in the distribution of ore elements along the cross-sections of all boreholes: (a) the Ni/Cu ratios decrease in the rocks with depth; (2) the Pd/Pt ratios show sawtooth patterns, but, in general, they increase with depth, whereas typomorphic features are observed for each rock layer: (a) Ni/Cu is more than one in picritic gabbro-dolerite, whereas Ni/Cu is less than one in olivine gabbro-dolerite; (b) contents of ore elements prevail in taxite gabbro-dolerites compared to picritic ones (Figure 3b–d), while they are higher in picritic gabbro-dolerite than in the underlying olivine gabbro-dolerite. The positive anomalies of Cu, Ni, Pt, Pd in picritic rocks coincide with the chromite layer (Figure 3d,g,h). This testifies to the independence of the melts from which each of the ore-containing rocks crystallized.

All chondrite-normalized patterns of elements distribution (noble metals, Ni, Co and Cu in 100% sulfide) in the disseminated ores of gabbro-dolerites correlate well with each other. All the curves are characterized by a positive Pd anomaly. The content of ore elements in 100% sulfide in picritic gabbro-dolerite somewhat predominates over that in olivine or taxite gabbro-dolerites (Figure 9a,b). The pattern of ore elements in the low sulfide horizon is characterized by higher contents of Pt and Pd, and is comparable with the data on J-M Reef [36].

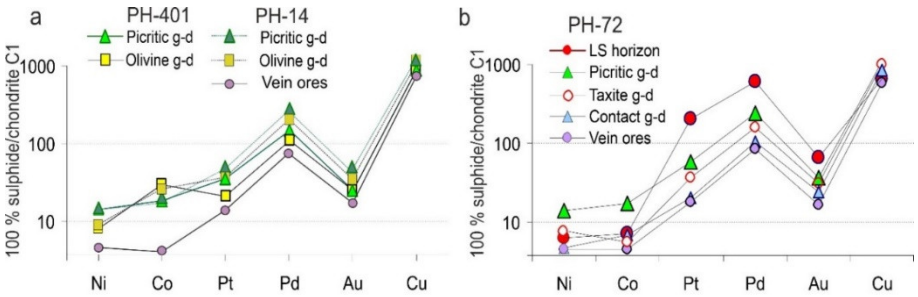

Figure 9. Average compositions of ore elements normalized to chondrite C1 [37]: (**a**) boreholes in which the lower layered series is represented by olivine gabbro-dolerites; (**b**) boreholes in which the lower layered series is represented by taxite gabbro-dolerites.

Chondrite-normalized patterns of PGEs from various types of rocks containing disseminated sulfide ores of the MOH (Table 4) show an upward trend zone from Os to Pd (Figure 10). This zone has a steeper slope compared to the distribution patterns from the Great Dyke, which indicates a higher degree of fractionation of PGEs in the primary sulfide melts of Norilsk 1.

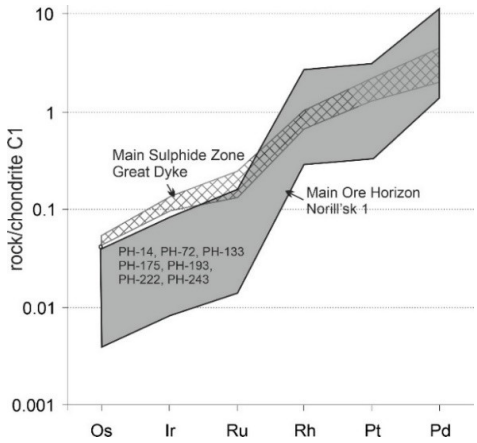

Figure 10. PGE content in the Main Ore Horizon, normalized to chondrite C1 [37], compared with the Great Dyke [38].

5.2. Mineralogical Features of Rocks

Iron-nickel ratios in pentlandite reflect the activity of sulfur ($lgfS_2$) during its formation [39–41]. The content of Ni in pentlandite increases as $lgfS_2$ increases. The Ni/Fe ratio in pentlandite increases with depth in MOH. The variation in k = Ni/(Ni + Fe) in pentlandite from borehole PH-14 varies in the range of 0.33−0.47 in picritic gabbro-dolerite, which corresponds to $lgfS_2$ from −12 to −11, whereas the variation in k in pentlandites from olivine gabbro-dolerite varies from 0.49 to 0.57; therefore, they are crystallized under the conditions of $lgfS_2$, corresponding to an interval from −10.5 to −9 [33]. The data from other boreholes also shows that pentlandite in picritic gabbro-dolerite has a higher content of Fe: k is 0.37 (PH-243), 0.45 (PH-175), 0.49 (PH-72 and PH-401) on average. Consequently, they crystallized with less S fugacity compared to pentlandites from olivine gabbro-dolerite (k is 0.52 in PH-401 and 0.47 in PH-243) or in taxite gabbro-dolerite (k is 0.48 in PH-72 and k is 0.56 in PH-175).

Thus, two different sulfide assemblages are characteristic of picritic and taxite (or olivine) gabbro-dolerites. The sequence of sulfide formation in picritic gabbro-dolerite is due to the sequential crystallization of a monosulfide solid solution (mss) and then a copper-rich residual melt, from which an intermediate solid solution (iss) was formed in the conditions of low sulfur fugacity. The solid-phase reactions with decreasing temperature led to the mss decomposition and the formation of an association of troilite, in which the plates of cubanite and Fe-rich pentlandite are present. This association then reacted then with the residual melt with an increase in the amount of cubanite up to the formation of granular species. Chalcopyrite, at this stage of crystallization was present in a sharply subordinate amount. Iss decomposed in association with chalcopyrite + Fe-rich pentlandite ± talnachite ± bornite ± cubanite ± $pyrrhotite_{(h > m)}$. (h—hexagonal, m—monoclinic). These studied parageneses in picritic gabbro-dolerite are related to the "low-sulfur" minerals sequence [1].

In olivine and taxite gabbro-dolerites, sulfides are represented by a "high-sulfur" association composed of $pyrrhotite_{(m > h)}$, (m—monoclinic, h—hexagonal) chalcopyrite, $pentlandite_{(Fe < Ni)}$ (Fe rich or Ni rich) and pyrite, which are due to the pyrrhotite-chalcopyrite fractionation in conditions of increased sulfur fugacity. At the same time, talnakhite, bornite, and native copper are absent in this assemblage. According to [4], these ores are characterized by the simple zonality of the first type. The sequence of crystallization of mineral parageneses is due to the evolution of mss and iss. When cooled, mss decomposes into monoclinic and hexagonal pyrrhotite with lamellas of chalcopyrite. According to the experimental data, tetragonal and cubic chalcopyrite and pentlandite with a high content of Ni are decomposed from iss [42]. The general sequence of sulfide formation of these ores was described by [1] based on the studies of [10,43].

Therefore, there is a clear genetic relationship between the sulfide assemblages in disseminated ores and the type of the host gabbro-dolerites. Our data show that the concentric zoning of the ores described by [4] is absent in the Norilsk 1 intrusion. In each rock layer (picritic, taxite or olivine gabbro-dolerites), the mineral associations do not change laterally, and are similar in the central part of the intrusion and in its flanks. Each of the stratigraphic layers has its own geochemical and mineral zoning from top to bottom, expressed by a decrease in the Ni/Cu ratio and an increase in the Pd/Pt ratio, the chalcopyrite share and the content of Ni in pentlandite. The general vertical zoning, despite the apparent continuity of geochemical characteristics, is actually composed of individual zoning. The apparent general zoning of the Main Ore Horizon is most likely superimposed, and the "continuity" is due to the fact that the layer underlying picritic gabbro dolerites (taxite or olivine gabbro-dolerites) was crystallized from a more fractionated silicate melt, which also contained a more fractionated sulfide liquid, from which the high-sulfur parageneses were crystallized.

Table 4. Compositions of rocks (with refractory PGE) of sample samples from core samples.

No	Borehole	Pt	Pd	Rh	Ru	Ir	Os	No	Borehole	Pt	Pd	Rh	Ru	Ir	Os
1	PH-14	0.94	2.16	0.082	0.024	0.008	0.003	48	PH-133	1.16	3.47	0.059	0.003	0.005	0.002
2	PH-14	0.45	1.16	0.059	0.020	0.007	0.002	49	PH-133	1.72	4.95	0.068	0.003	0.005	0.002
3	PH-14	0.77	2.04	0.159	0.037	0.014	0.005	50	PH-133	0.64	1.78	0.025	0.004	0.002	0.002
4	PH-14	0.41	1.38	0.088	0.023	0.008	0.003	51	PH-175	0.91	1.76	0.119	0.044	0.015	0.005
5	PH-14	1.27	3.86	0.597	0.265	0.086	0.029	52	PH-175	0.97	2.15	0.161	0.060	0.020	0.007
6	PH-14	3.88	5.30	0.762	0.064	0.055	0.018	53	PH-175	0.61	1.74	0.099	0.036	0.011	0.004
7	PH-14	0.73	1.95	0.062	0.017	0.009	0.003	54	PH-175	2.10	4.86	0.318	0.097	0.035	0.012
8	PH-14	1.37	3.03	0.172	0.011	0.012	0.006	55	PH-175	2.33	6.02	0.304	0.100	0.033	0.014
9	PH-14	0.85	2.37	0.109	0.034	0.012	0.004	56	PH-175	1.79	3.38	0.171	0.050	0.017	0.006
10	PH-14	1.55	4.32	0.183	0.056	0.018	0.006	57	PH-175	0.65	2.17	0.097	0.028	0.009	0.002
11	PH-14	0.42	1.61	0.046	0.014	0.004	0.002	58	PH-175	2.17	5.59	0.335	0.112	0.039	0.013
12	PH-14	0.33	0.96	0.048	0.012	0.005	0.002	59	PH-175	3.10	5.59	0.339	0.111	0.039	0.013
13	PH-14	0.75	2.28	0.048	0.010	0.005	0.002	60	PH-193	0.46	1.24	0.077	0.031	0.010	0.007
14	PH-14	0.52	1.78	0.058	0.015	0.005	0.002	61	PH-193	0.51	1.46	0.073	0.029	0.010	0.003
15	PH-14	1.45	2.20	0.069	0.021	0.006	0.002	62	PH-193	0.50	1.31	0.069	0.028	0.009	0.006
16	PH-14	0.32	1.13	0.044	0.011	0.004	0.002	63	PH-193	0.46	1.15	0.068	0.019	0.008	0.004
17	PH-14	0.36	1.63	0.130	0.040	0.011	0.004	64	PH-193	0.58	1.31	0.086	0.029	0.010	0.005
18	PH-14	4.10	13.09	0.321	0.037	0.026	0.009	65	PH-193	0.54	1.25	0.069	0.021	0.006	0.004
19	PH-72	1.22	2.77	0.214	0.059	0.027	0.009	66	PH-193	0.44	1.42	0.087	0.026	0.009	0.008
20	PH-72	0.56	1.34	0.098	0.040	0.012	0.004	67	PH-193	0.39	1.13	0.076	0.022	0.007	0.003
21	PH-72	15.28	21.41	0.345	0.122	0.038	0.013	68	PH-193	0.49	1.34	0.055	0.016	0.006	0.004
22	PH-72	0.73	1.64	0.111	0.042	0.016	0.005	69	PH-193	0.32	0.99	0.052	0.014	0.006	0.004
23	PH-72	0.81	3.01	0.130	0.045	0.016	0.002	70	PH-193	0.31	1.13	0.045	0.017	0.009	0.003
24	PH-72	1.55	3.84	0.249	0.076	0.027	0.002	71	PH-193	0.56	0.93	0.080	0.020	0.012	0.005
25	PH-72	1.53	4.75	0.267	0.085	0.030	0.010	72	PH-193	0.35	0.76	0.054	0.018	0.008	0.002
26	PH-72	0.38	1.33	0.053	0.017	0.005	0.002	73	PH-193	0.44	1.45	0.059	0.021	0.007	0.002
27	PH-72	0.44	1.56	0.056	0.015	0.006	0.002	74	PH-193	0.69	2.56	0.072	0.021	0.009	0.003
28	PH-72	1.47	3.33	0.328	0.148	0.043	0.002	75	PH-193	0.50	1.66	0.065	0.025	0.008	0.003
29	PH-72	2.67	8.78	2.489	1.376	0.410	0.004	76	PH-193	0.69	1.98	0.102	0.035	0.011	0.004
30	PH-72	0.82	2.56	0.085	0.004	0.006	0.002	77	PH-193	0.66	1.89	0.086	0.028	0.009	0.003
31	PH-72	2.38	5.98	0.339	0.119	0.041	0.017	78	PH-193	0.36	1.08	0.062	0.021	0.005	0.002
32	PH-72	2.19	5.72	0.312	0.099	0.039	0.007	79	PH-193	0.98	4.87	0.034	0.006	0.002	0.002

Table 4. *Cont.*

No	Borehole	Pt	Pd	Rh	Ru	Ir	Os	No	Borehole	Pt	Pd	Rh	Ru	Ir	Os
33	PH-133	0.71	1.91	0.127	0.036	0.015	0.004	80	PH-193	8.73	14.45	0.130	0.012	0.005	0.002
34	PH-133	0.55	1.33	0.085	0.022	0.010	0.002	81	PH-193	2.46	5.46	0.176	0.013	0.013	0.010
35	PH-133	0.56	1.35	0.078	0.024	0.009	0.002	82	PH-222	1.37	3.38	0.23	0.07	0.03	0.01
36	PH-133	1.31	3.94	0.175	0.053	0.018	0.002	83	PH-222	1.95	4.45	0.21	0.06	0.03	0.02
37	PH-133	0.62	1.74	0.130	0.043	0.012	0.006	84	PH-222	1.93	4.71	0.21	0.06	0.02	0.01
38	PH-133	1.09	2.25	0.154	0.044	0.015	0.002	85	PH-222	0.47	1.80	0.05	0.02	0.01	0.00
39	PH-133	0.75	2.11	0.123	0.036	0.011	0.002	86	PH-222	0.78	1.72	0.07	0.02	0.01	0.00
40	PH-133	1.13	3.08	0.218	0.071	0.022	0.007	87	PH-222	1.36	4.32	0.30	0.09	0.03	0.02
41	PH-133	1.71	5.47	0.306	0.097	0.030	0.010	88	PH-222	0.94	2.45	0.07	0.03	0.01	0.00
42	PH-133	1.48	3.52	0.125	0.053	0.014	0.005	89	PH-222	0.76	1.93	0.08	0.03	0.01	0.00
43	PH-133	15.06	17.50	0.261	0.101	0.027	0.009	90	PH-222	0.94	2.42	0.09	0.03	0.01	0.00
44	PH-133	0.78	2.75	0.039	0.011	0.004	0.002	91	PH-222	0.81	2.15	0.10	0.05	0.02	0.01
45	PH-133	0.81	1.75	0.056	0.001	0.002	0.002	92	PH-222	0.51	2.10	0.06	0.03	0.01	0.00
46	PH-133	0.33	1.13	0.055	0.001	0.005	0.002	93	PH-222	0.32	1.08	0.04	0.01	0.00	0.00
47	PH-133	0.38	1.46	0.027	0.019	0.004	0.002	94	PH-222	0.49	1.65	0.09	0.03	0.00	0.00

Since the ore-bearing horizons of the Norilsk 1 intrusion contain sulfur that exceeds its solubility in silicate magma by several times [44–46], it can be assumed that immiscible sulfide liquid as droplets in a silicate melt came from the mantle [47] or lower-crustal [3] chambers to the chamber of formation. The contrasting difference in the evolution of mineral paragenesis in picrite and taxite/olivine gabbro-dolerites may indicate two non-simultaneous melt pulses for these two types of mineralized rocks, providing the typomorphic features of each of the horizons. In other words, taxite and picritic gabbro-dolerites cannot be fractionated from a single melt in the formation chamber (intrusive body), but are the result of a two-stage magma injection of various melt types containing sulfide liquids of different compositions. The dissolution rates of sulfide droplets in flowing magma are slow relative to the flow rates, such that sulfide might be transported in, and deposited from, silicate magmas at distances of kms from the generation site [48]. This is consistent with the results for the U-Pb ages of zircons of the Kharaelakh intrusion (and, quite probably, others) that fit into four time intervals: 347 ± 16, 265.7 ± 11, 253.8 ± 1.7 and 235.7 ± 6.1 Ma [49], which indicates the multiphase introduction of melts. In addition, significant variations in εHf for different rocks of the Norilsk 1 intrusion suggest different sources that correspond to the parameters of varying degrees of interaction between the crust and the lithospheric mantle [49].

Vein-disseminated ores in the exocontact intrusion differ in their composition from overlying disseminated ores by the prevalence of pyrrhotite, and have higher contents of PGE: up to 10 ppm in borehole PH-222, and up to 20 ppm—in borehole PH-193 (Figure 3c,d). Therefore, these ores cannot be the result of the sedimentation of droplets at the bottom, as is assumed in the model. An alternative model suggests that the sulfide liquid was segregated from the silicate magma elsewhere and that this sulfide liquid was later injected between the consolidated intrusive and sedimentary rocks [50,51].

6. Conclusions

Thus, the following conclusions have been established on the basis of the mineralogical and geochemical features that:

1. The Ni/Cu ratios are decrease in each stratigraphic layer of rocks, and from picritic toward olivine (or taxite) gabbro-dolerites as a whole, in agreement with the increase in chalcopyrite in this direction;
2. The Ni/Fe ratios in pentlandite increase from top to bottom in each layer, and from picritic toward olivine (or taxite) gabbro-dolerites and to massive ores, which indicates an increase in sulfur fugacity in the mineral parageneses down the section of the borehole;
3. There is a clear correlation between the sulfide assemblages and the type of the host gabbro-dolerites: picritic gabbro-dolerites are characterized by a low-sulfur and Cu-rich sulfide assemblage; olivine and taxite gabbro-dolerites are characterized by a high-sulfur assemblage of sulfides. The differences in the types of mineralization are due to the particular compositions of sulfide melts and the different physicochemical conditions of their fractionation;
4. Taxite and picritic gabbro-dolerites cannot be fractionated from a single melt in the formation chamber, but are the result of a two-stage magma injection of various portions containing sulfide liquids of different compositions.
5. Vein-disseminated ores in the contacts of intrusions are not the result of the deposition of sulfide droplets at the place of formation, but are due to their later injection.

Author Contributions: N.T. conceived and designed the study, interpreted the results, and wrote this article. G.S. prepared detailed descriptions of numerous ore samples. A.P. provided the chemical analyses of the rocks and edited the manuscript. V.K. provided the analyses of minerals made on the WDS spectrometer. All authors have read and agreed to the published version of the manuscript.

Funding: This study was carried out within the framework of the state assignment of the VS Sobolev Institute of Geology and Mineralogy of the Siberian Branch of the Russian Academy of Sciences (financed by the Ministry of Science and Higher Education of the Russian Federation). We also acknowledge the financial assistance provided by the Novageo LLC, projects nos 10/17.

Acknowledgments: The authors are heartily grateful to the geologists of Russian Platinum LLC and to the head of the sector of the Testing and Analytical Center of Gipronickel Institute LLC., N.P. Shikhareva. The authors thank V.N. Knyazev (Siberian Federal University) for their help in analyzing data on an X-ray spectral microanalyzer, as well as chief geologist S.A. Zemlyanskiy and mineralogist P.N. Samorodskiy (LLC Novageo) for their assistance in processing samples.

Conflicts of Interest: The authors declare no conflict of interest.

References

1. Naldrett, A.J. *Magmatic Sulphide Deposits: Geology, Geochemistry and Exploration*; Springer: Berlin/Heidelberg, Germany; New York, NY, USA, 2004; p. 496.
2. Likhachev, A.P. *Platinum-Copper-Nickel and Platinum Deposits*; Eslan: Moscow, Russia, 2006; p. 496. (In Russian)
3. Krivolutskaya, N.A. *Evolution of Trap Magmatism and Processes Producing Pt-Cu-Ni Mineralization in the Noril'sk Area*; The Association of scientific publications, KMK: Moscow, Russia, 2014; p. 325. (In Russian)
4. Distler, V.V.; Genkin, A.D.; Filimonova, A.A.; Hitrov, V.G.; Laputina, I.P. The Zoning of Copper-Nickel Ores of Talnakh and Oktyabr'sky Deposits. *Geol. Ore Depos.* **1975**, *2*, 16–27. (In Russian)
5. Distler, V.V.; Nikol'skaya, N.N.; Yeshkova, Z.A. Elements of the platinum group in the traps of the Noril'sk region. In *Ore-Forming Elements of Basic and Ultrabasic Rocks*; Barnes, H.L., Ed.; Publishing House: Moscow, Russia, 1976; pp. 110–128. (In Russian)
6. Distler, V.V.; Malevsky, A.Y.; Laputina, I.P. Distribution of PGE between Pyrrhotite and Pentlandite during Crystallization of Sulphide Melt. *Geochemistry (Geokhimiya)* **1977**, *11*, 1646–1659.
7. Distler, V.V.; Kulakov, A.A.; Sluzhenikin, S.F.; Laputina, I.P. Quenched Sulphide Solid Solutions in Noril'sk Ores. *Geol. Ore Depos.* **1996**, *38*, 41–53. (In Russian)
8. Genkin, A.D.; Muravyova, I.V.; Troneva, N.V. Zvyagintsevite, the Natural Inter-Metallic Composition of Palladium, Platinum, Lead and Tin. *Geol. Ore Depos.* **1966**, *8*, 94–100. (In Russian)
9. Genkin, A.D.; Evstigneeva, T.L.; Troneva, N.V.; Vyalsov, L.N. Polarite Pd (Pb, Bi)—A New Mineral of Copper-Nickel Sulphide Ores. *Zap. VMO* **1969**, *98*, 708–715. (In Russian)
10. Genkin, A.D.; Distler, V.V.; Gladyshev, G.D.; Filimonova, A.A.; Evstigneeva, T.L.; Kovalenker, V.A.; Smirnov, A.V.; Grokhovskaya, T.L. *Sulphide Copper-Nickel Ores of the Noril'sk Deposits*; Nauka: Moscow, Russia, 1981; p. 374. (In Russian)
11. Genkin, A.D.; Evstigneeva, T.L. Associations of Platinum-Group Minerals of the Noril'sk Copper-Nickel Sulphide Ores. *Econ. Geol.* **1986**, *81*, 1203–1212. [CrossRef]
12. Begizov, V.D.; Meschankina, V.I.; Dubakina, L.S. Palladoarsenide Pd_2As—The New Native Palladium Arsenide from the Copper-NCkel Ores of Oktyabr'sky Deposit. *Zap. VMO* **1974**, *16*, 1294–1297. (In Russian)
13. Razin, L.V.; Dubakina, L.S.; Dubinchuk, V.T. Rhombic Palladium, Copper and Platinum Stannide from Copper-Nickel Sulphide Ores of Noril'sk-Type Deposits. Notes of the All-Union Mineralogical Society. *Zap. VMO* **1976**, *105*, 206–213. (In Russian)
14. Evstigneeva, T.L.; Genkin, A.D. Cabriite Pd_2SnCu, a New Species in the Mineral Group of Palladium, Tin and Copper Compounds. *Can. Mineral.* **1983**, *21*, 481–487.
15. Barkov, A.; Martin, R.; Poirier, G.; Tarkian, M.; Pakhomovskii, Y.; Men'shikov, Y. Tatyanaite, a New Platinum-Group Mineral, the Pt Analogue of Taimyrite, from the Noril'sk Complex (Northern Siberia, Russia). *Eur. J. Mineral.* **2000**, *12*, 391–396. [CrossRef]
16. Barkov, A.; Martin, R.; Poirier, G.; Yakovlev, Y. The Taimyrite-Tatyanaite Series and Zoning in Intermetallic Compounds of Pt, Pd, Cu, and Sn from Noril'sk, Siberia, Russia. *Can. Mineral.* **2000**, *38*, 599–609. [CrossRef]
17. Barnes, S.J.; Cox, R.A.; Zeintec, M.L. Platinum-Group Element, Gold, Silver and Base Metal Distribution in Compositionally Zoned Sulphide Droplets-Like Inclusions from Medvezhy Creek Mine, Noril'sk, Russia. *Contrib. Miner. Pet.* **2006**, *152*, 187–200. [CrossRef]
18. Spiridonov, E.M.; Kulagov, E.A.; Kulikova, I.M. Platinum and Palladium-Bearing Tetraauricupride and Associated Minerals in the Ores of the Noril'sk-I Deposit. *Geol. Ore Depos.* **2003**, *45*, 261–271. (In Russian)
19. Spiridonov, E.M.; Kulagov, E.A.; Kulikova, I.M. Association of Minerals of Palla-Dium, Platinum and Gold in Ores of the Noril'sk Deposit. *Geol. Ore Depos.* **2004**, *46*, 175–192. (In Russian)
20. Spiridonov, E.M. The Ore-Magmatic System of the Noril'sk Ore Field. *Russ. Geol. Geophys.* **2010**, *51*, 1059–1077. [CrossRef]

21. Duran, C.J.; Barnes, S.-J.; Plese, P.; Prasek, M.K.; Zientek, M.L.; Page, P. Fractional Crystallization-Induced Variations in Sulphides from the Noril'sk-Talnakh Mining District (Polar Siberia, Russia). *Ore Geol. Rev.* **2017**, *90*, 326–351. [CrossRef]
22. Tolstykh, N.; Krivolutskaya, N.; Safonova, I.; Shapovalova, M.; Zhitova, L.; Abersteinerd, A. Unique Cu-Rich Sulphide Ores of the Southern-2 Orebody in the Talnakh Intrusion, Noril'sk Area (Russia): Geochemistry, Mineralogy and Conditions of Crystallization. *Ore Geol. Rev.* **2020**, *122*, 103525. [CrossRef]
23. Ryabov, V.V. About composition of upper horizons of the Norilsk intrusions with rich chromite mineralization. In *Criteria of Ore Potential of Magmatic Rocks*; Nauka: Novosibirsk, Russia, 1984; pp. 124–142. (In Russian)
24. Distler, V.V.; Grokhovskaya, T.L.; Evstigneeva, T.L.; Sluzhenikin, S.F.; Filimonova, A.A.; Dyuzhikov, O.A. *Petrology of Magmatic Sulphide Ore Formation*; Nauka: Moscow, Russia, 1988; p. 232. (In Russian)
25. Sluzhenikin, S.F. Platinum-Copper-Nickel and Platinum Ores of Noril'sk Region and Their Ore Mineralization. *Russ. J. Gen. Chem.* **2011**, *81*, 1288–1301. [CrossRef]
26. Sluzhenikin, S.F.; Distler, V.V.; Dyuzhikov, O.A.; Kravtsov, V.F.; Kunilov, V.E.; Laputina, I.P.; Turovtsev, D.M. Low-Sulphide Platinum Mineralization in the Noril'sk Differentiated Intrusions. *Geol. Ore Depos.* **1994**, *36*, 195–217. (In Russian)
27. Sluzhenikin, S.F.; Distler, V.; Grigoryeva, A. Petrology of low-sulphide PGE ores of the Noril'sk region. In Proceedings of the 12th SGA Biennial Meeting, Uppsala, Sweden, 12–15 August 2013; pp. 1058–1060.
28. Sluzhenikin, S.F.; Krivolutskaya, N.A.; Rad'ko, V.A.; Malitch, K.N.; Distler, V.V.; Fedorenko, V.A. Ultramafic-mafic intrusions, volcanic rocks and PGE-Cu-Ni sulphide deposits of the Noril'sk province, Polar Siberia. Field trip guidebook. In *12th International Platinum Symposium*; Simonov, O.N., Ed.; IGG UB RAS: Yekaterinburg, Russia, 2014; p. 87.
29. Sluzhenikin, S.F.; Distler, B.B.; Grigoryeva, A.V. Low-Sulphide Platinum Ores of the Noril'sk Region—Promising Sources of Precious Metals. *Arct. Ecol. Econ.* **2016**, *4*, 32–45. (In Russian)
30. Tolstykh, N.; Zhitova, L.; Shapovalova, M.; Chayka, I. The evolution of the Ore-Forming System in the Low Sulfide Horizon of the Noril'sk 1 Intrusion, Russia. *Miner. Mag.* **2019**, *83*, 673–694. [CrossRef]
31. Komarova, M.Z.; Kozyrev, S.M.; Simonov, O.N.; Lyul'ko, V.A. The PGE mineralization of disseminated sulphide ores of the Noril'sk-Taimyr Region. In *The Geology, Geochemistry, Mineralogy and Mineral Beneficiation of Platinum-Group Elements*; Cabri, L.J., Ed.; Metallutry and Petroleum: Montreal, QC, Canada, 2002; Volume 54, pp. 547–567.
32. Kozyrev, S.M.; Komarova, M.Z.; Emelina, L.N.; Oleshkevich, O.I.; Yakovleva, O.A.; Lyalinov, D.V.; Maximov, V.I. The mineralogy and behaviour of PGM during processing of the Norilsk-Talnakh PGE-Cu-Ni ores. In *The Geology, Geochemistry, Mineralogy and Mineral Beneficiation of Platinum-Group Elements*; Special vol. 54; Cabri, L.J., Ed.; Canadian Institute of Mining, Metallurgy and Petroleum: Montreal, QC, Canada, 2002; pp. 757–791.
33. Tolstykh, N.D.; Shvedov, G.I.; Polonyankin, A.A.; Zemlyansky, S.A. Mineralogical and geochemical feature of the disseminated ores of the southern part of the Noril'sk 1 deposit. *IOP Conf. Ser. Earth Environ. Sci.* **2017**, *110*, 012021. [CrossRef]
34. Distler, V.V.; Sluzhenikin, S.F.; Cabri, L.J.; Krivolutskaya, N.A.; Turovtsev, D.M.; Golovanova, T.I.; Mokhov, A.V.; Knauf, V.V.; Oleshkevich, O.I. The Platinum Ore of the Noril'sk Layered Intrusions: The Ratio of Magmatic and Fluid Content of Noble Metals. *Geol. Ore Depos.* **1999**, *41*, 241–265. (In Russian)
35. Korolyuk, V.N.; Usova, L.V.; Nigmatulina, E.N. On the Accuracy of Determining Composition of Principal Rock-Forming Silicates and Oxides with a Jeol JXA-8100 Electron Microprobe. *J. Anal. Chem.* **2009**, *64*, 1070–1074. [CrossRef]
36. Godel, B.; Barnes, S.-J. Platinum-Group Elements in Sulfide Minerals and the Whole Rocks of the JM Reef (Stillwater Complex): Implication for the Formation of the Reef. *Chem. Geol.* **2008**, *248*, 272–294. [CrossRef]
37. Tagle, R.; Berlin, J. A Database of Chondrite Analyses Including Platinum-Group Elements, Ni Co, Au, and Cr: Implications for the Identification of Chrondritic Pro-Jectiles. *Meteorit. Planet. Sci.* **2008**, *43*, 541–559. [CrossRef]
38. Oberthur, T. Platinum-group element mineralization of the Great Dyke, Zimbabwe. In *The Geology, Geochemistry, Mineralogy and Mineral Beneficiation of Platinum-Group Elements*; Special vol. 54; Cabri, L.J., Ed.; Canadian Institute of Mining, Metallutry and Petroleum: Montreal, QC, Canada, 2002; pp. 483–506.
39. Kaneda, H.; Takenouchi, S.; Shoji, T. Stability of Pentlandite in the Fe–Ni–Co–S System. *Miner. Depos.* **1986**, *21*, 169–180. [CrossRef]

40. Kolonin, G.R.; Orsoev, D.A.; Sinyakova, E.F.; Kislov, E.V. Using the Ratio Ni:Fe in Pentlandite to Assess the Volatility in the Formation of Sulphur-Containing PGE Sulphide Mineralization of the Yoko-Dovyren Massif. Rep. *Russ. Acad. Sci. (Dokl. RAN)* **2000**, *370*, 87–91. (In Russian)
41. Kosyakov, V.I.; Sinyakova, E.F.; Shestakov, V.A. The Dependence of Fugacity of Sulphur from the Composition of Phase Associations of Fe–FeS–NiS–Ni at 873°K. *Geochemistry (Geokhimiya)* **2003**, *7*, 730–740. (In Russian)
42. Kosyakov, F.I.; Sinyakova, E.F.; Distler, V.V. Experimental Simulation of Phase Relationships and Zoning of Magmatic Nickel-Copper Sulphide Ores. *Russ. Geol. Ore Depos.* **2012**, *54*, 179–208. [CrossRef]
43. Dyuzhikov, O.A.; Distler, V.V.; Strunin, B.M.; Mkrtychyan, A.K.; Sherman, M.L.; Sluzhenikin, S.F.; Lurye, A.M. Geology and Ore Potential of the Noril'sk Ore District. Nauka, Moscow, 1988. (In Russian). Translated. Geology and metallogeny of Sulphide Deposits Noril'sk Region USSR. *Econ. Geol. Monogr. 1. Ont.* **1992**, *1*, 262.
44. Almukhamedov, A.I.; Medvedev, A.Y. *Sulfur Geochemistry in the Evolution of Basic Magmas*; Nauka: Moscov, Russia, 1982; p. 148. (In Russian)
45. Yang, X.-M. Sulphur Solubility in Felsic Magmas: Implications for Genesis of Intrusion-Related Gold Mineralization. *Geosci. Can.* **2012**, *39*, 17–32.
46. Lightfoot, P.S. Nickel Sulfide Ores and Impact Melts: Origin of the Sudbury Igneous Complex Presents a Current State of Understanding on the Geology and Ore Deposits of the Sudbury Igneous Complex in Ontario, Canada. *Elsevier Sci.* **2017**, *112*, 1543.
47. Likhachev, A.P. Formation of folded belts and possibility of a presence in them of PGE-Cu-Ni deposits. In Proceedings of the Mafic-ultramafic complexes of folded regions and related deposits, Kachkanar, Russia, 27 August–1 September 2009; pp. 24–26. (In Russian).
48. Barnes, S.J.; Robertson, J.C. Time Scales and Length Scales in Magma Flow Pathways and the Origin of Magmatic Ni-Cu-PGE Ore Deposits. *Geosci. Front.* **2019**, *10*, 77–87. [CrossRef]
49. Malich, K.N.; Badanina, I.Y.; Tuganova, E.V. *Ore-Bearing Ultramafic-Mafic Intrusives of Polar Siberia: Age, Conditions of Formation, Forecast Criteria*; IGG UB RAS: Yekaterinburg, Russia, 2018; p. 287. (In Russian)
50. Zen'ko, T.E.; Czamanske, G.K. Spatial and Petrologic Aspects of the Intrusions of the Noril'sk and Talnakh Ore Junctions. *Ont. Geol. Surv. Spec. Publ.* **1994**, *5*, 263–282.
51. Barnes, S.; Lightfoot, P. Formation of magmatic nickel sulfide deposits and processes affecting their copper and platinum group element contents. In *Economic Geology*; Hedenquist, J., Thompson, J., Goldfarb, R., Richards, J., Eds.; Society of Economic Geologist: Littleton, CO, USA, 2005; pp. 179–213.